NORSAR

ROYAL NORWEGIAN COUNCIL FOR SCIENTIFIC AND INDUSTRIAL RESEARCH

Scientific Report No. 2–76/77

SEMIANNUAL TECHNICAL SUMMARY

1 October 1976 – 31 March 1977

Edited by
H. Bungum

Kjeller, 15 March 1977

SECURITY CLASSIFICATION OF THIS PAGE *(When Data Entered)*

REPORT DOCUMENTATION PAGE		READ INSTRUCTIONS BEFORE COMPLETING FORM
1. REPORT NUMBER F08606-77-C-0001	2. GOVT ACCESSION NO.	3. RECIPIENT'S CATALOG NUMBER
4. TITLE *(and Subtitle)* Semiannual Technical Summary		5. TYPE OF REPORT & PERIOD COVERED Semiannual Tech. Summary 1 October 1976-31 March 1977 6. PERFORMING ORG. REPORT NUMBER Scientific Rep. 2-76/77
7. AUTHOR*(s)* H. Bungum (Editor)		8. CONTRACT OR GRANT NUMBER*(s)* F08606-77-C-0001
9. PERFORMING ORGANIZATION NAME AND ADDRESS NTNF/NORSAR Post Box 51, N-2007 Kjeller, Norway		10. PROGRAM ELEMENT, PROJECT, TASK AREA & WORK UNIT NUMBERS NORSAR Phase 3
11. CONTROLLING OFFICE NAME AND ADDRESS		12. REPORT DATE 15 March 1977 13. NUMBER OF PAGES 67
14. MONITORING AGENCY NAME & ADDRESS*(if different from Controlling Office)* VELA Seismological Center 312 Montgomery Street Alexandria, Virginia 22314		15. SECURITY CLASS. *(of this report)* 15a. DECLASSIFICATION/DOWNGRADING SCHEDULE

16. DISTRIBUTION STATEMENT *(of this Report)*

APPROVED FOR PUBLIC RELEASE; DISTRIBUTION UNLIMITED

17. DISTRIBUTION STATEMENT *(of the abstract entered in Block 20, if different from Report)*

18. SUPPLEMENTARY NOTES

19. KEY WORDS *(Continue on reverse side if necessary and identify by block number)*

20. ABSTRACT *(Continue on reverse side if necessary and identify by block number)*

This report describes the operation and research activities at the Norwegian Seismic Array (NORSAR) for the period from 1 October 1976 to 31 March 1977. The operation of the array in this period has been dominated by the effects of the change from 22 to 7 subarrays. There have been 232 breaks in the operation of the Detection Processor (DP), 121 of which have been due to SPS malfunctioning. Moreover, many of the breaks are tied to tests and software changes connected to the transition to a 7

DD FORM 1 JAN 73 1473 EDITION OF 1 NOV 65 IS OBSOLETE

SECURITY CLASSIFICATION OF THIS PAGE *(When Data Entered)*

subarray operation. The uptime has nevertheless been 95.5%, which is quite good in consideration of the fact that the operation is now unmanned except for weekday daytimes. Part of the explanation for this is an effective countermeasure in terms of an automatic telephone warning system triggered by DP stops. The gradual transition towards unmanned operation has been accompanied by the lay-off of 8 of the 9 computer operators, who have had little problems in finding new jobs. The performance of the data communications lines inside the array as well as within the ARPA subnetwork has been relatively satisfactory. Preliminary results on the performance of the new Online Event Processor (which is still being developed) indicate quite satisfactory results. A considerable amount of work has been invested in modifying and improving the DP. The work has partly been general system changes, and in particular those caused by the reduction in array size (including the development of the Online EP), and partly changes connected to the adaption of a new VELANET protocol for tran-Atlantic message exchange. The field work connected to the closing down of the 15 subarrays is now in progress, in accordance with a detailed plan. The work continues with getting attenuated LP data in parallel for all remaining subarrays. Some modifications have been made to the analog SP station, and one attenuated SP channel has been implemented. The regular array maintenance activity has been kept at its usual level, and the monitoring schedule has been adapted to the new array configuration.

The research activities are documented here in eleven reports covering a wide range of subjects. The first three reports cover further investigations of the crustal and lithospheric structure under NORSAR, by using the spectral ratio method in studying Moho depths under NORSAR (1), by using relative amplitude and travel time anomalies simultaneously in a new and encouraging approach on investigating lithospheric heterogeneities (2), and by using S to P refracted waves in finding the boundary between the lithosphere and the asthenosphere (3). The following three reports cover some aspects of seismicity; one report presents focal mechanism solutions for two recent earthquakes from Iceland and Svalbard (4), in another report the seismicity in the Svalbard area is further investigated, including an analysis of the crustal structure there (5), and the third seismicity investigation is from the Hindu Kush-Pamir region, where also the lithosphere has been investigated (6). Then follows a report on the P-wave detectability of a large number of WWSSN stations (7), a new approach on investigating microseismic noise using autoregressive modelling (8), and an important contribution to seismic discrimination where a pattern recognition approach has been developed (9). The following report describes a new method for estimation of spectral properties of spatial data (10), and the last one is a short note on the problem of estimating the autocorrelation function of spatio-temporal variables (11).

AFTAC Project Authorization No.	:	VELA VT/7702/B/ETR
ARPA Order No.	:	2551
Program Code No.	:	7F10
Name of Contractor	:	Royal Norwegian Council for Scientific and Industrial Research
Effective Date of Contract	:	1 October 1976
Contract Expiration Date	:	30 September 1977
Contract No.	:	F08606-77-C-0001
Project Manager	:	Nils Marås (02) 71 69 15
Title of Work	:	The Norwegian Seismic Array (NORSAR) Phase 3
Amount of Contract	:	$712.907
Contract Period Covered by the Report	:	1 October 1976 - 31 March 1977

This research was supported by the Advanced Research Projects Agency of the Department of Defense and was monitored by AFTAC, Patrick AFB FL 32925, under contract no. F08606-77-C-0001.

NORSAR Contribution No. 228

TABLE OF CONTENTS

TABLE OF CONTENTS (cont.)

I. SUMMARY

This report describes the operation and research activities at the Norwegian Seismic Array (NORSAR) for the period from 1 October 1976 to 31 March 1977.

The operation of the array in this period has been dominated by the effects of the change from 22 to 7 subarrays. There have been 232 breaks in the operation of the Detection Processor (DP), 121 of which have been due to SPS malfunctioning. Moreover, many of the breaks are tied to tests and software changes connected to the transition to a 7 subarray operation. The uptime has nevertheless been 95.5%, which is quite good in consideration of the fact that the operation is now unmanned except for weekday daytimes. Part of the explanation for this is an effective countermeasure in terms of an automatic telephone warning system triggered by DP stops. The gradual transition towards unmanned operation has been accompanied by the lay-off of 8 of the 9 computer operators, who have had little problems in finding new jobs. The performance of the data communications lines inside the array as well as within the ARPA subnetwork has been relatively satisfactory. Preliminary results on the performance of the new Online Event Processor (which is still being developed) indicate quite satisfactory results. A considerable amount of work has been invested in modifying and improving the DP. The work has partly been general system changes, and in particular those caused by the reduction in array size (including the development of the Online EP), and partly changes connected to the adaption of a new VELANET protocol for trans-Atlantic message exchange. The field work connected to the closing down of the 15 subarrays is now in progress, in accordance with a detailed plan. The work continues with getting attenuated LP data in parallel for all remaining subarrays. Some modifications have been made to the analog SP station, and one attenuated SP channel has been implemented. The regular array maintenance activity has been kept at its usual level, and the monitoring schedule has been adapted to the new array configuration.

The research activities are documented here in eleven reports, covering a wide range of subjects. The first three reports cover further investigations of the crustal and lithospheric structure under NORSAR, by using the spectral ratio method in studying Moho depths under NORSAR (1), by using relative amplitude and travel time anomalies simultaneously in a new and encouraging approach on investigating lithospheric heterogeneities (2), and by using S to P refracted waves in finding the boundary between the lithosphere and the asthenosphere (3). The following three reports cover some aspects of seismicity; one report presents focal mechanism solutions for two recent earthquakes from Iceland and Svalbard (4), in another report the seismicity in the Svalbard area is further investigated, including an analysis of the crustal structure there (5), and the third seismicity investigation is from the Hindu Kush-Pamir region, where also the lithosphere has been investigated (6). Then follows a report on the P-wave detectability of a large number of WWSSN stations (7), a new approach on investigating microseismic noise using autoregressive modelling (8), and an important contribution to seismic discrimination where a pattern recognition approach has been developed (9). The following report describes a new method for estimation of spectral properties of spatial data (10), and the last one is a short note on the problem of estimating the autocorrelation function of spatio-temporal variables (11).

H. Bungum

II OPERATION OF ALL SYSTEMS

II.1 Detection Processor (DP) Operation

Within the reporting period there have been 232 breaks in the otherwise continuous operation of the Detection Processor (DP) system. The uptime percentage is 95.5%, as compared to 96.6% for the last reporting period (July-September 1976). Fig. II.1 and the accompanying Table II.1.1 both show the daily DP downtime, in hours, for the days between 1 October 1976 and 31 March 1977. The monthly recording times and up percentages are given in Table II.1.2.

As can be seen from Fig. II.1, there are days with long downtime intervals towards the end of the period. In most cases, these are stops that have occurred during unmanned shifts, when the automatic telephone alarm either was not yet installed or just failed. As experience is gained with the alarm system, we hope to improve its performance.

There were two breaks on 26 December, which were caused by power failure and Special Processing System (SPS) malfunctioning. These intervals together gave a total downtime of nearly 14 hours.

The 232 breaks occurring within the reporting period may be grouped in the following categories:

a)	SPS malfunctioning	121
b)	Error on the multiplexor channel	31
c)	Tests	17
d)	Software related stops	15
e)	Operation stops	13
f)	Maintenance	7
g)	CPU disabled	7
h)	Tape drive problems	6
i)	Power jumps and breaks	5
j)	Other hardware (TOD, Air condition)	4
k)	EOC unit problems	3
l)	Unknown	3

It is evident that the source of the major part of the breaks in the recording is the SPS. Since diagnostic aids are very limited for this system, it is difficult to track down any intermittent failures such as those occurring. (For futher information about the status of the SPS, see elsewhere in this report.)

The error on the multiplexor channel, which occurred in abundance in the beginning of this reporting period, has not occurred after the beginning of January. This is because the load on the multiplexor channel has been decreased, by moving the output for the printer to a tape on a selector channel instead, and also by reserving the multiplexor channel exclusively for ARPANET message traffic during unmanned shifts (as described under Improvements and Modifications). Thus we have virtually eliminated the occurrence of this error.

The rather high number of tests and software related stops (program changes and program errors) must be seen in relation to the system being in a state of transition throughout this period, with frequent modifications and improvements. Also, the technique of testing out the new versions of the system as the Secondary Online system (on the B-computer) before putting it into operation has been used very little, because of the risk of bringing down the SPS while initiating the Secondary Online system.

The category g) (CPU disabled) is almost certainly a hardware error, occurring while executing one of the microcodes on the A-computer. At least one of these cases was positively identified as such. All these stops have occurred within the last month, and further investigations will probably give more conclusive evidence.

The total downtime for this period was 204 hours 3 minutes. The mean-time-between-failures was 0.8 days as compared with 0.4 days for July-September 1976.

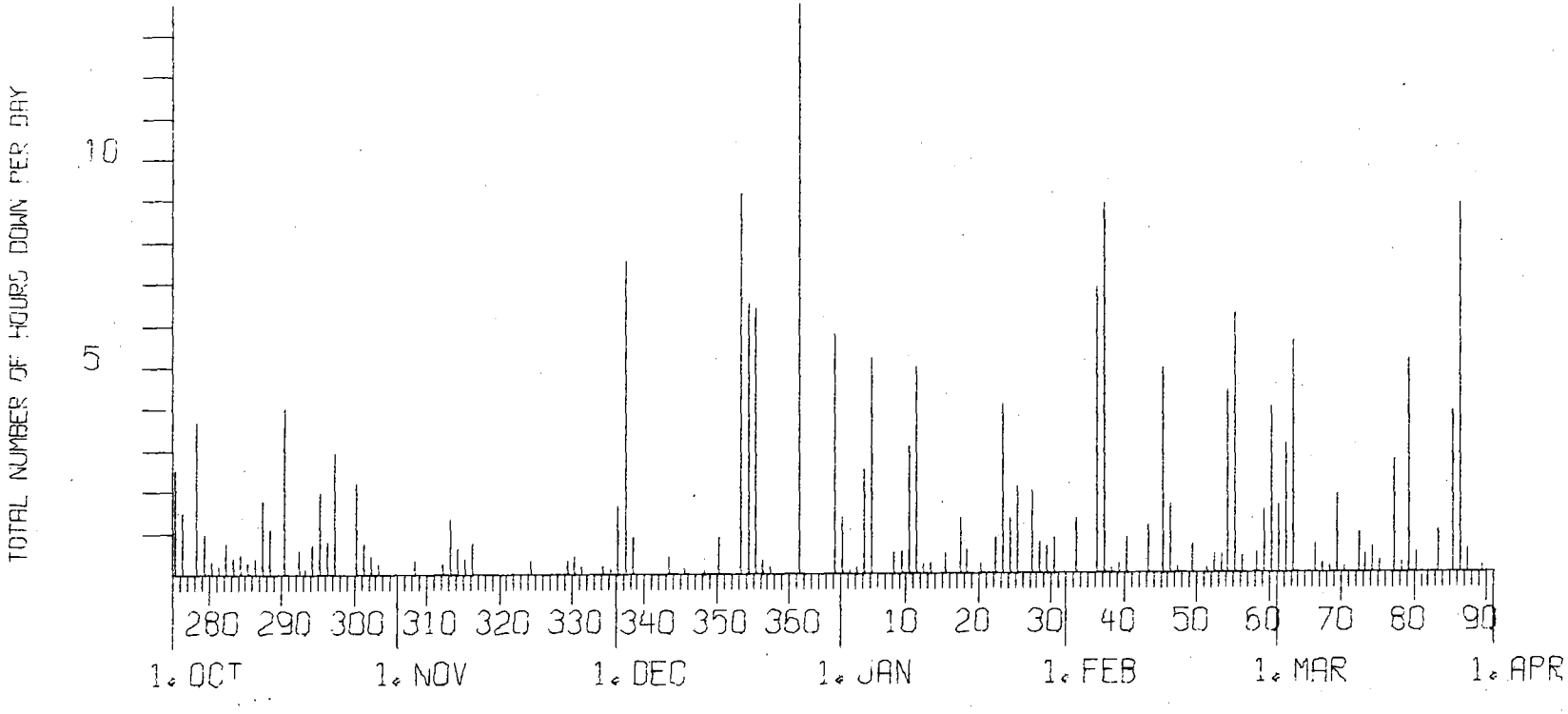

Fig. II.1 Detection Processor Downtime Oct 1976 - Mar 1977.

LIST OF BREAKS IN DP PROCESSING THE LAST HALF-YEAR

DAY	START		STOP		COMMENTS.....
275	0	32	2	6	MULTIPLEX/LATE ERROR
275	9	21	9	41	MULTIPLEX/LATE ERROR
275	22	26	23	2	MULTIPLEX/LATE ERROR
276	4	35	5	11	MULTIPLEX/LATE ERROR
276	5	39	5	52	MULTIPLEX/LATE ERROR
276	8	50	9	20	MULTIPLEX/LATE ERROR
276	15	55	16	5	MULTIPLEX/LATE ERROR
278	2	52	5	52	MULTIPLEX/LATE ERROR
278	13	5	13	32	PROG CHANGE
278	15	0	15	13	PROG CHANGE
279	5	13	5	29	MULTIPLEX/LATE ERROR
279	5	46	5	53	MULTIPLEX/LATE ERROR
279	7	26	7	36	MULTIPLEX/LATE ERROR
279	14	45	15	7	MULTIPLEX/LATE ERROR
280	12	10	12	16	PROG CHANGE
280	16	41	16	53	PROG CHANGE
281	0	0	0	10	MULTIPLEX/LATE ERROR
282	16	46	17	30	MULTIPLEX/LATE ERROR
283	15	15	15	39	MULTIPLEX/LATE ERROR
284	13	53	14	20	MULTIPLEX/LATE ERROR
285	13	31	13	48	PROG CHANGE
286	3	35	3	44	SPS
286	3	49	4	1	SPS
287	0	31	2	17	INCORRECT INITIALIZATION
288	0	33	1	6	INCORRECT INITIALIZE
288	12	50	12	53	MOVE PRINTOUT TO 1403
288	14	21	14	51	MULTIPLEX/LATE ERROR
290	8	6	10	7	SPS AND DISK DRIVE
290	10	29	12	26	SPS AND DISK DRIVE
292	14	20	14	53	PROG CHECK
293	12	9	12	15	SPS
294	5	30	5	45	POWER JUMP
294	6	31	6	41	SPS
294	10	0	10	17	SYSTLM TAKEN DOWN
295	9	47	9	57	SPS
295	11	19	12	19	SPS
295	22	37	22	53	SPS
295	23	30	24	0	SPS
296	0	0	0	18	SPS
296	9	9	9	38	SPS
297	18	0	20	55	SPS STOP (UNMANNED)
300	8	0	10	12	MAINTENANCE ON SPS
301	9	7	9	27	SPS
301	12	4	12	23	SPS
301	18	0	18	5	SPS

TABLE II.1.1

(Sheet 1 of 6)

LIST OF BREAKS IN DP PROCESSING THE LAST HALF-YEAR

DAY	START		STOP		COMMENTS.....
302	1	6	1	21	SPS
302	10	2	10	13	1052 MAINTENANCE
303	0	52	1	6	SPS
308	9	15	9	29	MOVE PRINTOUT TO 1403
308	14	11	14	16	MOVE PRINTOUT TO TAPE
312	17	0	17	15	SPS
313	0	8	0	34	SPS
313	9	39	10	10	SPS AND CHANGE THE 1052
313	23	37	24	0	SPS
314	0	0	0	8	SPS
314	3	4	3	13	SPS
314	13	12	13	30	SPS
315	5	6	5	27	PROG CHECK
316	2	43	3	7	SPS
316	18	1	18	21	SPS
324	11	8	11	15	MOVE PRINTOUT TO 1403
324	11	55	12	8	MOVE PRINTOUT TO TAPE
329	12	43	13	2	PROGRAM TEST
330	7	45	8	2	PROGRAM TEST
330	13	10	13	18	PROGRAM TEST
331	13	0	13	10	PROGRAM TEST
334	10	36	10	47	OPERATOR ERROR
335	8	6	8	13	SPS
336	10	18	10	33	POWER JUMP
336	14	39	14	45	EOC POWER ON
336	22	44	24	0	MPX/LATE (UNMANNED)
337	0	0	6	58	MPX/LATE (UNMANNED)
337	14	11	14	19	PROGRAM CHECK
337	23	34	24	0	MPX/LATE (UNMANNED)
338	0	0	0	52	MPX/LATE (UNMANNED)
343	8	52	9	3	PLOTTER MAINTENANCE
343	15	27	15	39	SPS
345	8	24	8	30	EOC DOWN
348	14	37	14	42	SPS MAINTENANCE
350	10	12	10	30	PROG CHECK
350	12	27	12	45	PROGRAM CHANGE
350	16	48	17	5	PROGRAM CHANGE
353	6	16	15	18	POWER SUPPLY MAINT.
353	16	21	16	29	EOC POWER ON
354	1	33	7	34	MPX/LATE
354	15	45	16	0	MPX/LATE
354	23	48	24	0	MPX/LATE
355	0	0	6	22	MPX/LATE
356	11	56	12	16	PROGRAM CHANGE
357	13	30	13	38	TOD CORRECTION
361	1	40	10	24	POWER BREAK
361	13	24	18	24	SPS
366	18	16	24	0	SPS

TABLE II.1.1

(Sheet 2 of 6)

LIST OF BREAKS IN DP PROCESSING THE LAST HALF-YEAR

DAY	START		STOP		COMMENTS.....
1	0	0	0	13	SPS
1	0	21	1	2	SPS
1	11	15	11	23	TIMING INCORRECT
1	18	5	18	23	TIMING INCORRECT
2	8	38	8	43	TIMING INCORRECT
3	9	15	9	24	PROGRAM CHANGE
4	10	32	10	47	SPS
4	14	41	14	51	MPX/LATE
4	18	27	20	14	SPS
4	20	21	20	40	SPS
5	0	58	6	8	SPS (UNMANNED)
8	21	27	21	57	SPS (ALARM)
9	16	41	16	48	SPS
9	22	21	22	46	SPS (ALARM)
10	7	30	8	54	SPS
10	9	43	10	53	SPS
10	20	30	20	39	PROG CHECK
11	1	45	5	50	POWER BREAK
11	6	42	6	56	SPS
11	13	38	13	51	PROGRAM CHANGE
11	17	48	18	14	TAPE DRIVE
12	11	14	11	27	UNKNOWN REASON
13	10	6	10	20	SPS
15	2	40	3	8	SPS (ALARM)
17	0	17	1	0	SPS (ALARM)
17	19	14	19	50	TAPE DRIVE CONTROLLER
18	8	20	8	43	SPS
18	10	15	10	18	SPS MAINTENANCE
18	12	7	12	12	SPS
20	12	4	12	17	SPS
22	21	7	21	37	SPS
22	22	35	22	53	SPS
23	0	13	2	30	SPS
23	6	7	6	44	SPS
23	8	10	8	25	SPS
23	8	49	9	16	SPS
23	10	26	10	37	SPS
23	16	35	16	54	SPS
24	14	16	14	32	SPS
24	16	19	16	53	SPS
24	23	6	23	35	SPS
25	8	15	9	44	SPS

TABLE II.1.1

(Sheet 3 of 6)

LIST OF BREAKS IN DP PROCESSING THE LAST HALF-YEAR

DAY	START		STOP		COMMENTS.....
25	13	13	13	33	SPS
25	13	46	14	2	SPS
27	6	11	7	38	AIR CONDITION FAILURE
27	8	33	9	5	TEMPERATURE HIGH
28	17	28	18	6	UNKNOWN REASON
28	18	45	18	51	UNKNOWN REASON
29	13	41	14	18	SPS
30	4	1	4	24	SPS
30	7	24	7	51	SPS
33	17	43	17	49	SPS ROS WORD
33	19	2	20	15	SPS ROS WORD
36	4	8	7	45	SPS (ALARM FAILURE)
36	8	18	8	36	SPS
36	21	3	24	0	SPS (ALARM FAILURE)
37	0	0	8	36	SPS (ALARM FAILURE)
37	17	22	17	40	SPS
38	12	58	13	3	SPS
39	9	11	9	23	SPS
40	6	1	6	12	SPS
40	11	6	11	11	SPS
40	14	24	14	37	SPS
40	21	42	22	4	SPS
43	1	24	1	57	SPS
43	16	16	16	51	SPS
45	2	31	2	50	SPS
45	9	14	9	20	SPS
45	9	24	11	28	SPS
45	14	27	15	21	SPS
45	16	1	16	9	SPS
45	19	5	19	15	SPS
45	20	39	21	34	SPS
45	23	27	23	46	SPS
46	8	28	9	43	SPS
46	16	46	16	54	SPS
46	17	38	17	49	SPS
46	20	30	20	36	SPS
47	17	34	17	41	SPS
49	3	53	4	15	SPS
49	7	1	7	10	SPS
49	9	21	9	26	SPS
49	11	24	11	28	SPS
51	11	5	11	12	SPS
52	6	33	6	58	TAPE DRIVE
53	6	7	6	27	TAPE DRIVE
53	17	50	17	55	SPS

TABLE II.1.1

(Sheet 4 of 6)

LIST OF BREAKS IN DP PROCESSING THE LAST HALF-YEAR

DAY	START		STOP		COMMENTS.....
54	13	13	13	23	SPS
54	18	51	22	12	SPS (ALARM FAILURE)
54	22	33	23	0	SPS
54	23	37	24	0	SPS (ALARM FAILURE)
55	0	0	6	4	SPS (ALARM FAILURE)
55	17	34	17	43	SPS
56	12	24	12	36	SPS
56	14	45	14	57	SPS
58	5	46	6	15	SPS
59	4	19	4	40	SPS
59	9	52	10	17	SPS
59	10	21	10	51	SPS
59	12	26	12	36	SPS
59	15	21	15	26	SPS
60	0	20	0	43	SPS
60	9	51	9	59	SPS
60	12	21	13	26	PROGRAM TEST
60	14	8	14	28	PROGRAM TEST
60	14	46	15	3	PROGRAM TEST
60	15	31	15	45	PROGRAM TEST
60	15	54	17	25	PROGRAM TEST
61	9	41	9	49	PROGRAM TEST
61	14	11	14	17	SPS
61	15	42	16	36	PROGRAM TEST
61	17	15	17	44	CPU DISABLED
62	13	16	15	47	PROGRAM TEST
62	17	46	18	21	PROGRAM TEST
63	6	14	7	33	TAPE DRIVE
63	12	32	12	45	PROGRAM TEST
63	13	50	15	6	PROGRAM TEST
63	15	28	17	59	PROGRAM TEST
63	18	8	18	22	PROGRAM TEST
66	12	35	13	16	CPU DISABLED
67	15	57	16	10	CPU DISABLED
68	14	23	14	31	SPS
69	4	36	6	17	HARDWARE ERROR
69	9	57	10	2	SWITCH COMPUTERS
69	10	22	10	27	SPS
70	9	6	9	12	SPS
72	8	29	8	41	CPU DISABLED
72	20	5	20	15	SPS
72	20	48	21	24	SPS
73	1	24	1	45	SPS
73	14	17	14	21	SPS MAINTENANCE
74	11	41	12	16	SPS
75	12	15	12	31	CPU DISABLED
77	14	15	15	51	CPU DISABLED
77	16	6	16	18	SPS

TABLE II.1.1

(Sheet 5 of 6)

LIST OF BREAKS IN DP PROCESSING THE LAST HALF-YEAR

DAY	START		STOP		COMMENTS.....
77	16	20	17	15	SPS
78	9	34	9	49	SPS
79	15	35	15	56	SPS
79	16	13	16	25	SPS
79	17	40	22	16	SPS MAINTENANCE
80	3	40	4	7	SPS
83	7	11	8	2	SPS
83	15	23	15	34	SPS
85	20	7	24	0	SPS (ALARM FAILURE)
86	0	0	8	53	SPS (ALARM FAILURE)
87	11	16	11	39	CPU DISABLED
87	13	36	13	46	POWER JUMP
89	8	40	8	49	TAPE DRIVES

TABLE II.1.1

(Sheet 6 of 6)

Month	DP Uptime (Hrs)	DP Uptime (%)	No. of DP Breaks	No. of Days with Breaks	DP MTBF* (Days)	EP Uptime (Hrs)	EP Uptime (%)
Oct	716.3	96.3	47	24	0.7	33.0	4.4
Nov	716.0	99.4	19	12	1.6	51.0	7.1
Dec	691.6	93.0	21	14	1.5	65.0	8.7
Jan	711.3	95.6	51	23	0.6	65.0	8.7
Feb	632.4	94.1	43	18	0.7	30.0	4.5
Mar	703.4	94.5	51	23	0.6	25.0	3.4
	4171.0	95.5	232	114	0.8	269.0	6.2

* Mean-time-between-failure

TABLE II.1.2

DP and EP Computer Usage October 76 - March 77

II.2 Event Processor (EP) Operation

The regular operation and maintenance of this system was discontinued after 1 October. However, some processing has still been done as can be seen from Table II.1.2.

D. Rieber-Mohn

II.3 NORSAR Data Processing Center (NDPC) Operation

Data Center

The reduction in the number of computer operators from 9 to 1 took place in the period, accompanied by a gradual change from manned to unmanned operation. Up to 20 November a full 24-hour shift plan was used with lack of operators for only a few shifts. From 20 November to 15 January there was manned operation in the period 0700 to 2200 throughout the week. The rest of the period there was manned operation from 0700 to 2200 Monday through Friday and 7 hours on Saturday and Sunday. As for the operators who had to leave, five were engaged as operators and one as a programmer at other data processing centers in the area.

In order to be able to restart the Detection Processor when it stops due to some failure in unmanned periods, an automatic calling device has been installed. When DP stops, the calling device is initiated and a telephone call is made to the person whose telephone number has been programmed into the calling device. This, together with some changes in the DP program, is the reason why DP uptime is as high as 95.5%.

Maintenance of computer equipment is in general still taken care of by subcontractors. Project personnel have, however, extended the area of participation and cover, in addition to the SPS and Experimental Operations Console (EOC), also Tape Units. Our aim is to reduce

the subcontractors' maintenance engagement, not only to special equipment like SPS, EOC, etc., but also tape unis, certain controllers and equipment with a high degree of reliability.

Data Communications

The number of subarrays was reduced from 22 to 7 on 30 September 1976 and the number of communications circuits was reduced accordingly. The performance of the remaining circuits has been relatively satisfactory, even though groups of subarrays have been affected by irregularities in carrier frequency equipment, power failures, etc.

Single subarray communication systems have been affected for other reasons, such as broken telephone cables, power failures, faulty equalizers, and heavy damping on special frequencies. These incidents normally caused longer outages. Subarrays which have been particularly affected are:

01A	Week	2/77	15% outage
01A	"	6/77	14% outage
02B	"	2/77	25.7% outage
02C	"	42,44/76	20.8 and 37.4% (reduced performance, < 200 errors per 16 2/3 minutes)
02C	"	51/76	22.8% -"-
02C	"	2/77	5.1% outage
02C	"	5,6/77	7.2, 8.6% (reduced performance, < 200 errors per 16 2/3 minutes)

The performance of the modems and other communications hardware has been satisfactory. In March 1977 the Central Terminal Vault (CTV) modem at 06C failed due to a faulty card. In order to improve the reliability of the existing communications system, the Norwegian Telegraph Administration (NTA) has remeasured all circuits and new equalizers/amplifiers will be installed.

Table II.3.1 indicates degraded performance and outages of the different subarray communications circuits.

Sub-array	Oct (4) >20	Oct (4) > 200	Nov (4) >20	Nov (4) >200	Dec (5) >20	Dec (5) >200	Jan (4) >20	Jan (4) >200	Feb (4) >20	Feb (4) >200	Mar (5) >20	Mar (5) >200	AVG ½ Year >20	AVG ½ Year >200
01A	0.3	0.5	1.0	0.5	0.1	0.1	0.2	4.0	0.4	11.2	0.2	0.2	0.4	2.8
01B	0.2	0.2	0.8	0.6	0.2	0.2	0.3	0.6	0.5	0.6	0.2	2.4	0.4	0.8
02B	0.1	0.3	0.8	0.5	-	1.7	0.1	6.9	0.3	0.6	0.2	0.2	0.3	1.7
02C	14.1	1.0	0.8	0.4	8.9	1.2	11.3	1.7	4.1	0.6	0.3	0.4	6.6	0.9
03C	0.1	0.3	1.1	0.4	0.1	-	0.2	0.4	0.6	0.5	3.5	0.5	1.0	0.4
04C	0.1	0.3	0.9	0.1	0.1	-	0.2	0.4	0.3	0.7	0.2	0.2	0.3	0.3
06C	0.2	0.4	0.9	0.6	0.1	0.1	0.1	1.0	0.3	0.8	1.9	5.2	0.6	1.4
AVG	2.2	0.4	0.9	0.4	1.4	0.5	1.8	2.1	0.9	2.1	0.9	1.3	1.4	1.2
Less	02C 0.2				02C 0.1		02C 0.2			01A 0.6			02C 0.5	

Table II.3.1

Communications, degraded performance (>20/outages >200). Figures in per cent of total time.

Month - 4 or 5 weeks as indicated.

The ARPA Subnetwork (TIP to TIP, i.e., TIP-modem/com. lines/ modem-TIP)

The London Circuit

The operation has been satisfactory apart from a few incidents with 'Carrier Loss', indications.

The SDAC Circuit

In October 1976 deteriorated data were reported relatively often. Tests and checks were run with participation of such agencies as NCC, ITT, and NTA. The rest of the reporting period was far more reliable, although 'Carrier Loss' and flashing in 'Marginal Circuit' indicators (both are modem indicators) were observed from time to time.

The Terminal Interface Message Processor (TIP) (Including Modems and Interfaces)

The TIP equipment operation has been satisfactory, apart from a period in October 1976 with particularly long outages. These outages were mainly caused by a Modem Interface (no. 1) where a defective card had to be replaced. In addition the CPU and the power supply cooling fans were out of operation, the former due to a blown fuse and the latter due to a burned field winding. Lack of cooling was the probable reason behind the Modem Interface trouble, which occurred in the period 22-25 October when the TIP, apart from relatively short periods, was down most of the time. Also 26 October was troublesome with respect to the TIP. There were several reasons for that: TIP crashed due to lost 'key-in-loader' (software). Also start button failed causing trouble when trying to read and restore 'key-in-loader'. In addition, Modem Interface No. 1 operation was intermittent and so was the SDAC communications line.

In December the TIP was turned off for 10 hours due to installation of a special 'Relay Supervising Unit' in the AC mains to the computer hall. At the same time the TIP power cable was replaced in order to protect the TIP system against longer power outages during unmanned periods (when 'Supervising Relay' operates and has to be reset manually), and because of the need for a power cable able to carry heavier loads.

Apart from incidents mentioned above, and minor trouble 4 November 1976 (due to software and a blown fuse in the SDAC modem), the TIP has performed well. The TIP has, of course, stopped later, but restart could be done in a straightforward manner most of the times. Average number of outages per month in the reporting period is 3.3.

J. Torstveit
O.A. Hansen

II.4 ARPANET

The Norwegian Defence Research Establishment (NDRE) has attached its system to the Very-Distant-Host (VDH) port during this period, and performed some measurements on this connection. However, regular operation of this system as a Host on the network has not yet started. Otherwise, the attachment configuration and the use of the ARPANET node has remained the same.

D. Rieber-Mohn

III. ARRAY PERFORMANCE

The regular operation of the old Event Processor was discontinued on 1 October 1976, when the array was reduced from 22 to 7 subarrays. At the same time, the production of the NORSAR Weekly Event Summary (or the seismic bulletin) was stopped. The EP system, which has demanded significant efforts both in terms of computer capacity and personnel will be replaced by an Online Event Processor (ONEP) which is still being developed. A preliminary version of the ONEP was implemented on 24 December 1976. In order to have some data available for the largest events, and in order to test the performance of the ONEP, the regular EP was operated from 19 October to 31 December 1976, and for some shorter intervals in January 1977. The Fast EP has also been used at several instances for interesting events, in particular presumed nuclear explosions.

We have conducted some analysis of the performance of the ONEP. In a comparison with the old EP (for part of December 1976) it was found to perform quite favorably. The beam reduction procedure is somewhat different (for example, the ONEP does not permit more than one processing or effort at each event), and the ONEP was not found to have more cases in which one missed the epicenter completely. The ONEP, of course, is bound to choose a beam location for each event (no refinement), but even this is not much of a problem since the location capability in most regions using only 7 subarrays is not much better than the average distance between beams. Using a random selection of about 25 events, it was found that the average location difference between ONEP and EP was less than 2^{o} both in latitude and longitude.

In looking separately at the ONEP results for the time period up to 1 March 1977, it was found that in average 10 events per day could easily be identified as either earthquakes

or explosions. Between 1 and 2 of these were located obviously incorrectly and would need to be processed over again if they should be used, say, for a seismic bulletin. For the purpose of testing and evaluation, the threshold was kept so low that an average of 27 events were selected and plotted each day. This could be done easily because the size of the plots has been reduced from 19(27) x 11 inches in the old EP to 5 x 10 inches in the Online EP.

H. Bungum
P. Engebretsen

IV IMPROVEMENTS AND MODIFICATIONS

IV.1 Detection Processor

The work on the Detection Processor system within this period may be separated into two (partially overlapping) categories:

a) general error corrections and system improvements, and

b) building a version of the system which is adapted to the new VELANET protocol for message exchange via the ARPA network, but which otherwise incorporates the old version.

Under category a), the following changes may be listed:

- Two new operator commands were added to the system in November. These commands make it possible to switch the output intended for the printer to a specially assigned tape ('noprt'), or back to the printer ('print'). The default option will be that printer output is written to tape, since this is more suitable for unmanned operations. Implementation of this set of operator commands required modifications in the code for the PNOPER2 and LNMSGR processors in the Message Task, as well as in the CASSGN-routine of the DP-Monitor. The CASSGN routine is now able to change assignments for non-tape devices as well, and to return the old assignment to the calling program. A new routine, SWTCHMSG, was introduced (as overlay NDPC2$25) in order to interpret the new set of commands and to call the CASSGN-routine accordingly.

- Changes were made to the PNRERR processor in November, so that the periodic Error Report now is printed for valid (i.e., remaining) subarrays only, and only if any error count for a valid subarray is nonzero.

- An improvement of the Host-Going-Down logic was done to the MONSER routine in the Network task. The routine now checks for 'Host-Going-Down' signalled from the Data Acquisition Task on every call (not only after a re-activation), and sends out the 'Host-Going-Down' message to the IMP before the system goes down.

- In December, the first version of the Online Event Processor was developed and implemented into the system. The introduction of this new processor as part of the Detection Task, with its parameter lists and buffers, required a re-organization of the core layout. A new phase was introduced, which contains the Tape, Detection and Network tasks. This phase is loaded during system initialization, but after the SPS blocks have been read from the Core Image tape and transferred to the SPS. The loading is done by PNRINT. Extra code was added to the PNHRTP processor, to extract high rate data from the High Rate Data Block and insert into the input buffer for the Online Event Processor. This processor, called PNREPX, was introduced into the Detection Task, and minor modifications and adjustments were made to other components of this task (SNDEPR, PNRICX, PNREDS). A new Core Image tape was prepared, incorporating parameters and buffers for the PNREPX processor.

- In accordance with the general philosophy of frugal tape use, the interval for writing LTA-data to the Detection Log tape was changed to 10 minutes (SNRDAQ).

- By the end of December, two new sets of operator commands were implemented. The first set enables the operator to start ('monit') and stop ('nomon') logging of outgoing ARPANET message headers onto the Detection Log tape, together with the time of write (to TIP) completion. (The Detection Log tape may then later be used as input for an off-line program to give information about the outgoing message flow.)

  The second operator command set implemented ('nomux', 'muxit') enables the operator to re-direct permanently all output intended originally for the 1052 console typewriter or the 2540 card punch, to the printer instead (or to the tape receiving printer output), or reversing this option. The 'nomux' command will be typed in at the

start of intervals of unattended operation, thus forcing all system status output to one (tape) unit, and leaving the multiplexor channel free for network traffic only. This also reduces considerably the probability of occurrence of a 'Multiplexor/Late' hardware error during unattended periods.

The new operator commands required changes in the PNOPER2 processor, as well as additions in the Message Task Local Common (LNMSGR). New subroutines (MONMSG and MUXMSG) for interpreting the commands were introduced as additional overlays (NDPC2$26 and NDPC2$27).

- An error in the PNRICX processor in the Detection task leading to incorrect end times for incoherent detections, was discovered and corrected in January. Also, detections having an LTA value equal to zero (occurring sporadically), were discarded (PNREDS).
- The Physical Unit Block (PUB) Table (AFMPUB) was expanded, in January, to its maximum of 22 entries. This allows a pool of 11 scratch tapes to be set up initially. Since only 3 tapes are in use at any time (High Rate, Low Rate and Det Log), this allows for an unattended period of more than 24 hours.

Under category b), (buildup of a new version), the following was done:

- The two-pass processor in the Detection Task (PNRSAD) that generates outgoing ARPANET messages and queues them to the Network Task, was completely re-designed. This was done in order to adhere to the new VELANET message format that will be used in the future, and also to transmit low gain long period data from one subarray, and optionally 20 Hz short period data from a requested instrument.

- In the Network (NCP) Task, minor changes were done to the IMPOUT, IMPWRITE and IMPREAD subtasks because of the new message lengths and formats. Also, Command Control Words (CCWs) in NCP Common (NCPCOMM) were changed because of this. In the IMPIN subtask, the logic for verifying an incoming VELANET message was changed to be in accordance with the new format. Also, extra logic was inserted to check for gaps in the sequence of incoming messages, and to check for re-initialization of the SDAC CCP (the VELANET header count is then zero), and to notify the SNNCPR sequencer on such occasions. This latter task was modified to be able to interpret the new intra-task signals and to convert them to messages to be queued to the High Priority Message Task. Also, the process of re-initialization of the complete task (and thereby the ARPANET-CCP connection) was diversified, so that the task may be re-initialized when desired without any wait time. This is contrary to the case for the 'Imp Going Down/Imp Dead' situation, where 2 minutes pass before re-initialization is done.

  Also, a new mechanism was built into the IMPTIM subtask to prevent hangups of the outgoing ARPANET message flow after, say, re-initialization of the TIP or Pluribus IMP (this situation occurs sporadically). The length of the time interval that has passed since the completion of the last write operation (to the TIP) is computed every time this subtask is activated (each minute). If this time interval exceeds a certain limit (say, 20 seconds), the SNNCPR subtask is signalled to perform a re-initialization of the complete task, thus restarting the write as well as the read operations.

- Additional logic has been inserted into the Online Event Processor (PNREPX) in order to, on the basis of the beam number of the event selected, to select and load an overlay module, containing a segment of a table of location

parameters for each beam number. The parameters in question are extracted and inserted into the Short Period Variable File (SPVF) section of the output buffer from this processor, along with status parameters collected from other parts of the system.

- The Message Task Common (LNMSGR) was expanded and modified to incorporate message skeletons for the necessary new system output messages. It was decided that it is better to send back a message explicitly spelling out the generated response of an SDAC data request message, or alternatively send back an error message, than merely unwittingly reflecting the request message, as has been done up to present. The SAACMMSG processor was therefore changed accordingly. The REFLECT segment was removed, while the REFORMAT segment was modified to give a more detailed confirmation message, or an error message, indicating the error in the request message.

- A mechanism for saving the last EPX number used by the Online Event Processor across system-down gaps has been implemented, thus maintaining a one-to-one correspondence between EPX number and processed events within, say, a year. This mechanism is implemented as follows: The Online Event Processor (PNREPX) will, when finding a new event, queue the EPX number of this event to the Disk Task. The Disk Task Sequencer (SNDISR) recognizes this type of queue block as one containing an EPX number and writes it to a special location on the Shared Disk Pack. Whenever the Disk Task performs initialization after system startup, it will read the EPX number from the location on the Shared Pack, add 10 and initialize the EPX counter in the Online Event Processor (PNREPX) with the result. In this way, it should be possible to avoid ambiguity with respect to using EPX numbers as event identificators within a period of, say, a year.

- New code for computing the number of subarrays down was inserted in the PNSADP and PNDKIR processors in the Disk Task.
- A table of location parameters (latitude, longitude, distance, azimuth, etc.) has been generated and split up into phase overlays, to be loaded from PNREPX. There is one entry for each beam number of each partition.

IV.2 Event Processor

This sytem has been adapted to used new format High Rate tapes as input.

D. Rieber-Mohn

IV.3 Array Instrumentation and Facilities

As of 1 October 1976 the communication lines to the fifteen subarrays to be closed down were switched off after prior notice to the local power companies and NTA. Landowners of nine of the CTV and LPV areas replied positively to a request of taking over the use of the vaults, including all responsibilities. The last six will then be completely sealed and secured with concrete. Up to now only the CTV/LPV at 11C have been sealed. The status of the array reduction program regarding the CTV/LPVs is given in the Table IV.3.1. All work on the WHVs is remaining and is planned completed during this year.

Transportation of the equipment from the CTV/LPVs to NMC is expected to take three to four weeks, starting in the beginning of May.

Sub-array	Equipment demounted	Equipment taken to NMC	Comments
03B	x	x	
04B	x *	x	Except LPV equipment
05B	x		
06B	x		
07B	x		
01C	x *		
05C	x *	x	
07C	x *	x	
08C	x *		
09C	x		
10C	x		
11C	x	x	Secured with concrete
12C	x		
13C	x		
14C	x		

* Concrete sealing remaining.

Table IV.3.1

Status of the array reduction work

Attenuated long period channels were installed at subarray 01B 24 November 1976. The output from all three LP seismometers are taken out in parallel with the normal data channels on the DB1 attenuator card, attenuated -40 dB and fed through separate Ithaco amplifiers through three additional LP Line Termination Amplifiers (LTA) (in positions A8 and A9 in SLEM) to multiplexer channels 30, 31 and 32 for Vertical, North-South and East-West components, respectively. The sampling rate is 0.5 Hz, sampled on Random Data Addresses (RDA) 13, 14 and 15 (refer Fig. IV.3.1). The test function routing is given in Table IV.3.2, and the MUX channels assignments in Table IV.3.3. The separate Ithacos are damping the seismometers with an average percentage of 12, and the damping resistances have been increased accordingly to compensate. Investigations have been initiated to improve the attenuation circuits, that is, to decrease the Ithaco gain and alter the attenuation circuit components for better damping effects.

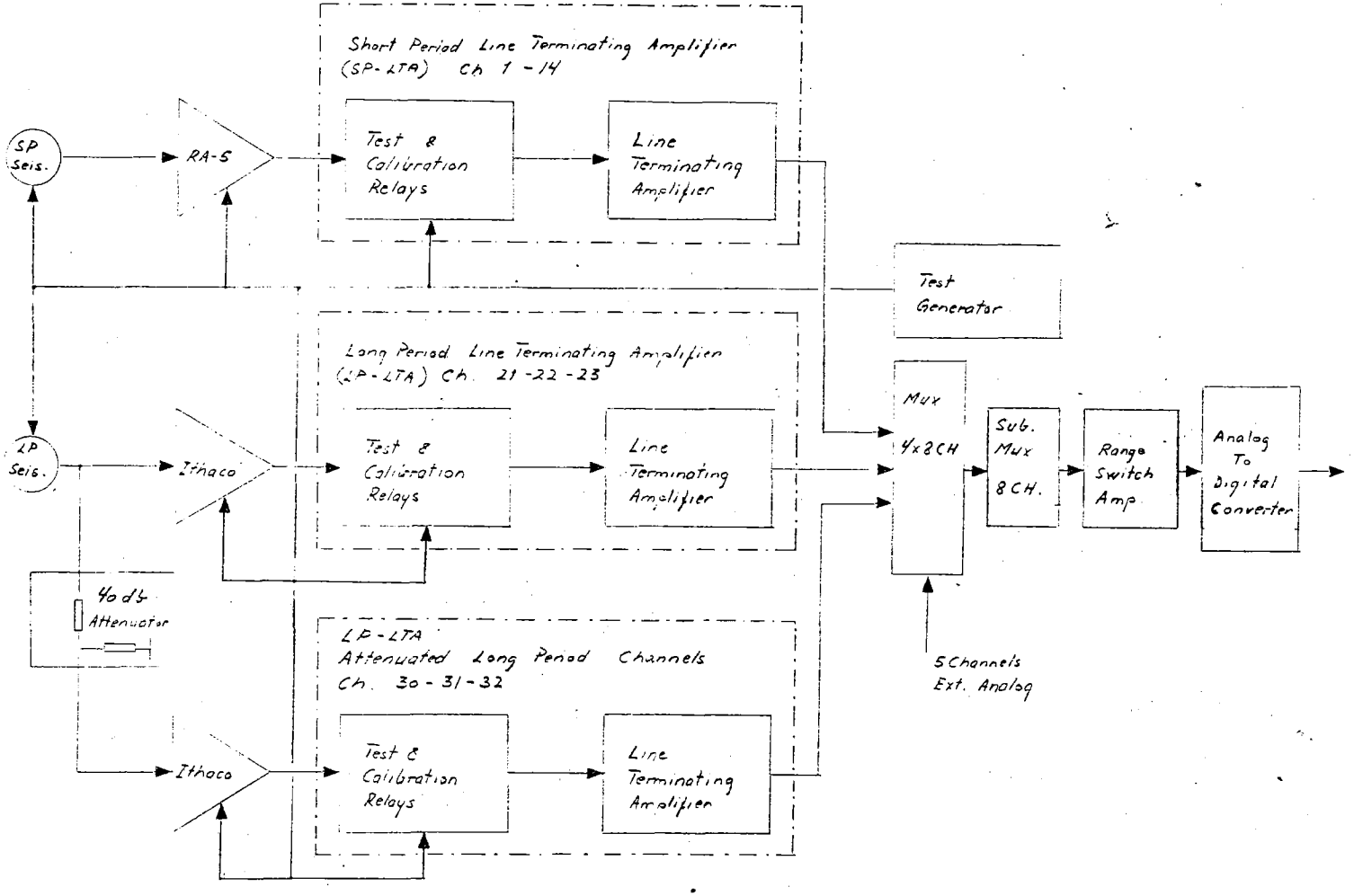

Fig. IV.3.1 Block diagram of 01B, including attenuated LP-channels.

Function Route Select FRA 2^5	2^4	2^3	2^2	2^1	2^0	Test Bus Connection
0	1	0	1	1	0	LTA No. 15 Vertical
0	1	0	1	1	1	LTA No. 16 North-South
0	1	1	0	0	0	LTA No. 17 East-West
0	1	0	0	1	1	LTA No. 18 Spare LP ch.

Table IV.3.2

Test Function Routing

Ch.	Signal	Mux Address
18	Spare LP	1 0 0 0 1
30	Vertical LP	1 1 1 0 1
31	North-South LP	1 1 1 1 0
32	East-West LP	1 1 1 1 1

RDA

Table IV.3.3

Mux Channels Assignment

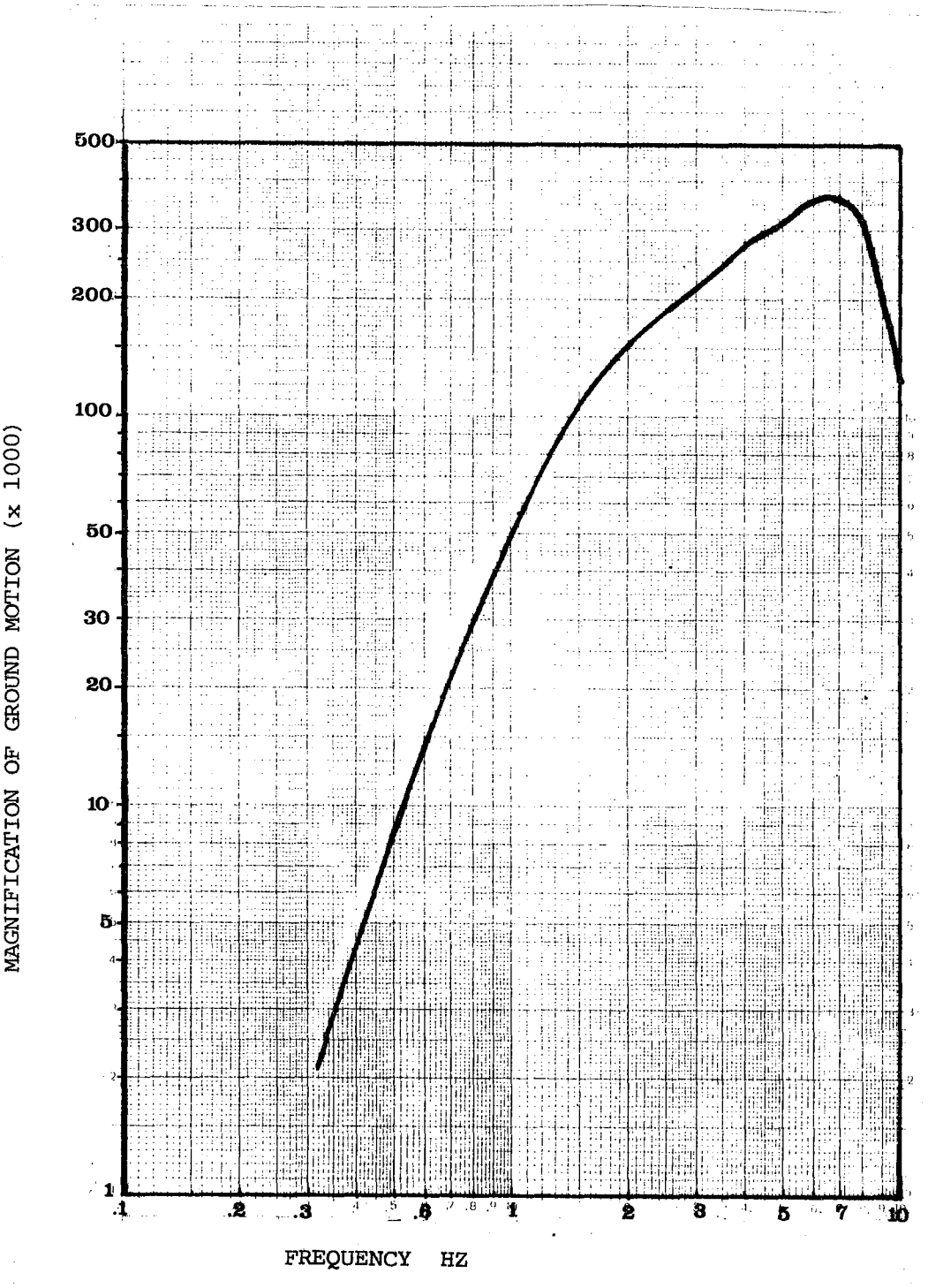

Fig. IV.3.3 Frequency response of NORSAR Analog SP Station 25 March 1977 (8.0 Hz filter).

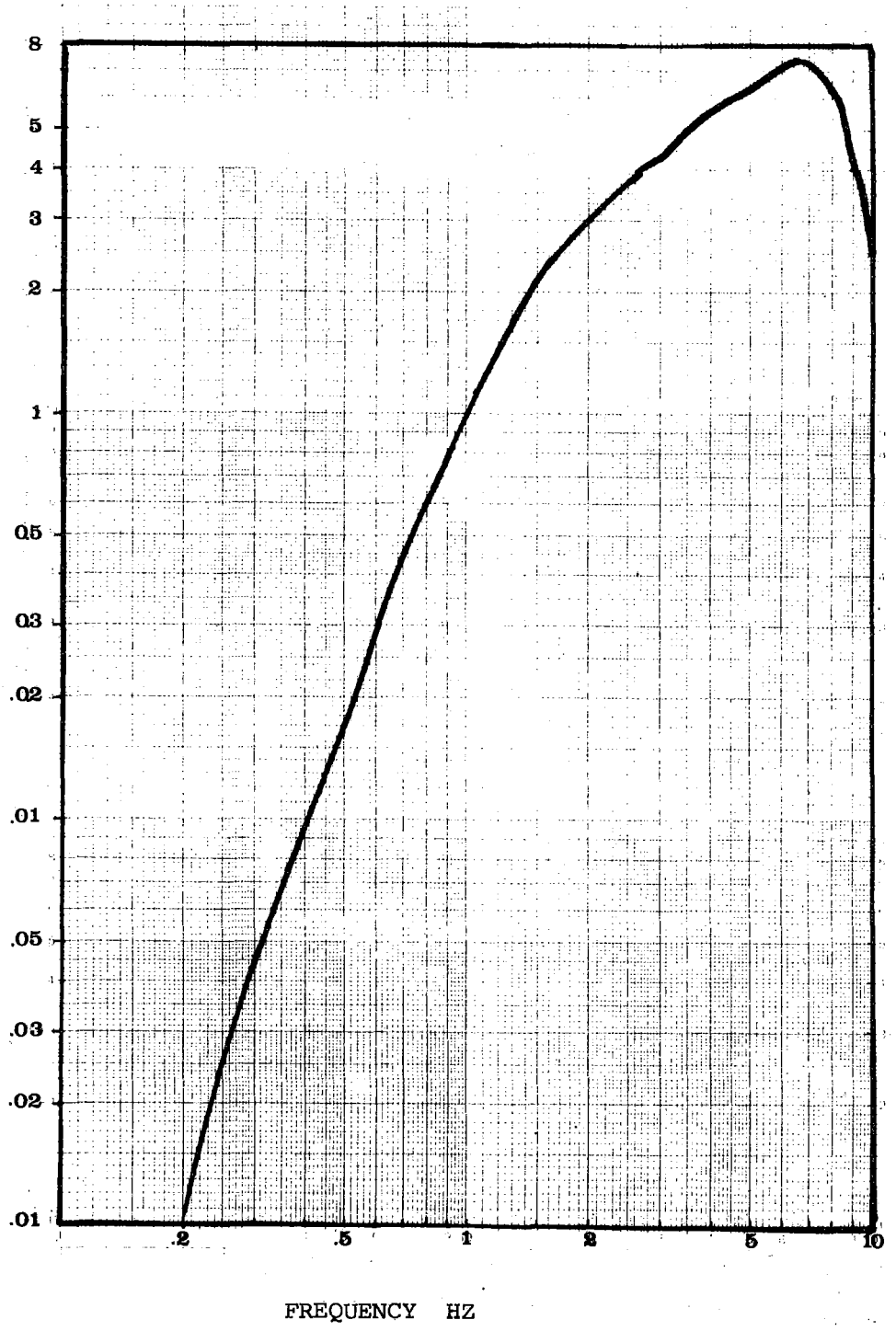

Fig. IV.3.4 Magnification of ground motion relative to magnification at 1.0 Hz of NORSAR Analog SP Station, March 1977.

A new Line Termination Amplifier with a filter of upper 3 dB point at 8.0 Hz was installed 25 March 1977 in the NORSAR Analog SP Station (refer Larsen, 1975). The frequency response after the installation are shown in Figs. IV.3.3 and IV.3.4, with the corresponding numbers given in Table IV.3.4.

For improved magnitude calculations for nearby large events the output from 01A06 seismometer was attenuated -30 dB and fed to channel 01A04 seismometer amplifier input (28 October 1976). Channel 01A06 operates as normal (Refer Fig. IV.3.2).

Alf Kr. Nilsen

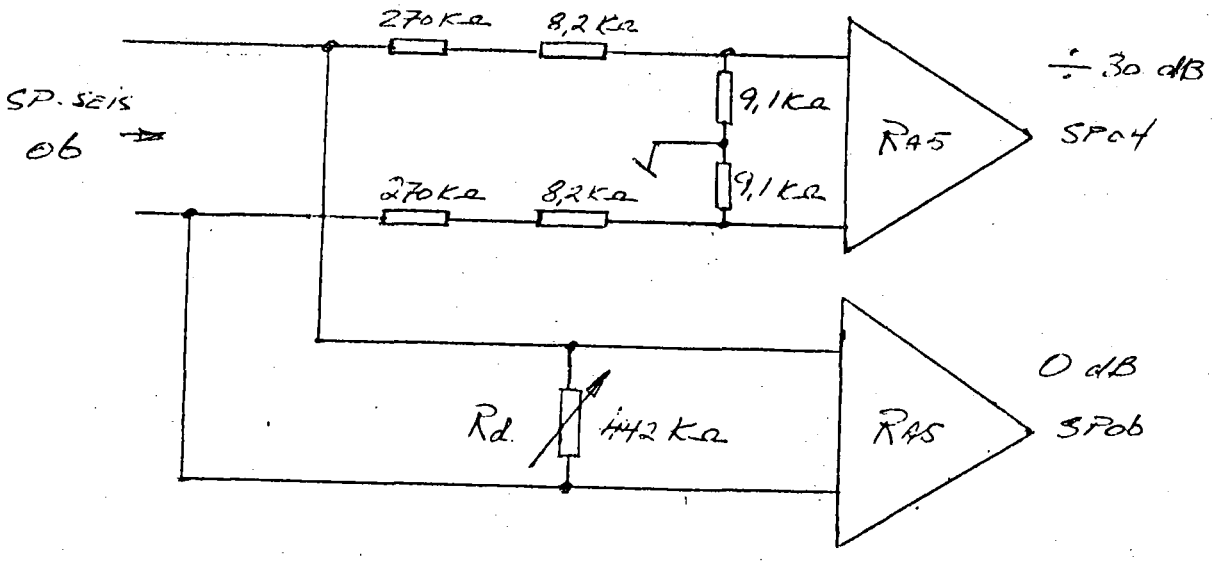

Fig. IV.3.2 Output from the seismometer at 01A06 from 28 October 1976.

Frequency Hz	Recoder Deflection mm	Magnification	Magnification Ratio relative to Magnification at 1 Hz
0.143	3.0	153	0.003
0.2	5.0	500	0.010
0.33	8.5	2312	0.046
0.5	13.0	8117	0.162
0.625	16.5	16098	0.322
0.8	19.0	30372	0.608
0.95	19.5	43956	0.878
1.0	20.0	49954	1.000
1.05	20.5	56451	1.130
1.25	20.0	78053	1.562
1.6	18.5	118291	2.368
2.0	15.0	149861	3.000
2.5	12.0	187327	3.750
3.0	9.5	213552	4.275
4.0	7.0	279741	5.600
5.0	5.0	312211	6.250
6.0	4.0	359667	7.200
7.0	3.0	367160	7.350
8.0	2.0	319704	6.400
8.5	1.5	270687	5.419
9.0	1.0	202313	4.050
9.5	0.75	169062	3.384
10.00	0.5	124884	2.500

$$M = \frac{a}{y}$$

$$y = \frac{G \cdot I \cdot 10^3}{4\pi^2 \cdot f^2 \cdot m}$$

where M = the seismograph magnification, λ = Damping 0.73, f_o = nat. frequency 1.05 Hz, I = Cal. current 400μA, a = peak-to-peak deflection in mm on the seismogram, y = equivalent ground motion in microns, m = seismometer mass 825 gr, G = cal. coil motor constant 0.0326 N/A, f = cal. frequency.

Table IV.3.4

Magnification of NORSAR Analog Station, 25 March 1977
(8 Hz filter)

V. MAINTENANCE ACTIVITY

A brief review of the maintenance accomplished at the subarrays by the field technicians as a result of the remote array monitoring and routine inspections is given. The monitoring schedule has been changed to fit the new array configuration, but the test frequency on the individual subarrays is little changed. Except for the array reduction work, all maintenance referred to is on the new array configuration.

Maintenance Visits

Fig. V.1 shows the number of visits to the subarrays in the period. Excluding maintenance visits on the communications system, the subarrays have on the average been visited 3.7 times. The subarrays in the new array configuration have been visited 3.1 times on the average (excluding 01B: 1.8 times), the large number of visits to 01B are due to cable breakage and installation of attenuated LP channels.

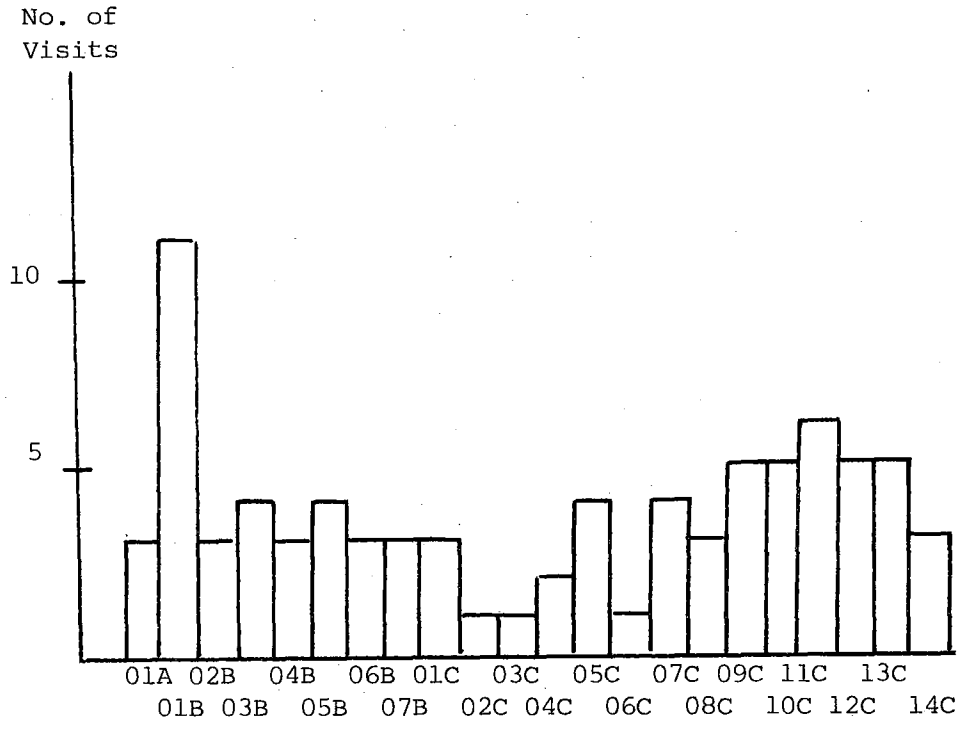

Fig. V.1 Number of visits to NORSAR subarrays 1 October 1976 - 31 March 1977.

Preventive Maintenance Projects

The preventive maintenance work in the new array is described in Table V.1.

Unit	Action	No. of Actions
LTA	Adjustment of SP DC offset	5
	Adjustment of channel gain SP	5
	Adjustment of channel gain LP	1
Power	Battery Maintenance	10

Table V.1

Preventive Maintenance Work in the Period
1 October 1976 - 31 March 1977

Disclosed Malfunctions on Instrumentation and Electronics

Table V.2 gives the number of accomplished adjustments and replacements of field equipment in the array with the exception of those mentioned in Table V.1.

Unit	Characteristic	SP		LP	
		Repl.	Adj.	Repl.	Adj.
Seis-mometer	RCD			3	
	Damping				5
Seis-mometer Ampli-fier (RA-5, Ithaco)	DCO			1	
LTA	Filter	1			
	Ch. gain		1		1
	CMR		1		
	DCO		3		
SLEM					
BB Gen.			1		
RSA/ ADC			1		
EPU		1			

Table V.2

Total number of required adjustments and replacements in the NORSAR data channels and SLEM electronics.

Malfunction of Rectifiers, Power Loss, Cable Breakages

There has been no malfunction of rectifiers in the period. Power loss requiring action by the field technicians or local power company are reported in Table V.3.

Sub-Array	Fault	Period of Inoperation	Comments
02B	No power at site	27-29 Nov 76	No line power
02B	-"-	12-14 Jan 77	-"-

Table V.3

Power Loss

One cable breakage (01B03) has been repaired requiring 13 days' work of the field technicians. The period of channel inoperation was from 11 October - 21 December 1976.

Conclusion

Compared with previous periods, the performance of the array instrumentation has been stable and satisfactory in this period. Though adjustment of SP channels DC offset to a small positive bias is part of the routine preventive work, the array average DC offset is now -4 millivolts, but no significant change of the drift rate towards negative offset is observed.

The NORSAR Analog SP station was set in operation again 9 November after installation of a new power supply system.

New versions of the analyzing programs were tested out in the first half of the period and catalogued on disk (N-5); CHANEVSP 30 November and CHANEVLP, SACP and MISNO as of 12 January 1977.

Alf Kr. Nilsen

References

Larsen, P.W. (1975): Reinstallation of NORSAR SP Analog station, NORSAR Internal Report No. 5-74/75, NTNF/NORSAR, Kjeller, Norway.

ABBREVIATIONS

ADC	-	Analog-to-Digital Converter
BB	-	Broad band
CMR	-	Common mode rejection
CTV	-	Central Terminal Vault
DC	-	Direct current
DCO	-	DC offset
EPU	-	External power unit
LP	-	Long period
LPV	-	Long period vault
LTA	-	Line Termination Amplifier
MP	-	Mass position
MUX	-	Multiplexer
NMC	-	NORSAR Maintenance Center
NTA	-	Norwegian Telegraph Administration
RA-5	-	SP seismometer amplifier
RCD	-	Remote centering device
RSA	-	Range switching amplifier
SLEM	-	Seismic short and long period electronics module
SP	-	Short period
WHV	-	Well head vault

VI. DOCUMENTATION DEVELOPED

VI.1 Reports, Papers

Berteussen, K.-A.: Final Report, NORSAR Phase 3, 1 July - 30 September 1976, NORSAR Scientific Report No. 1-76/77, NTNF/NORSAR, Kjeller, Norway.

Berteussen, K.-A.: Long period P-wave spectra as a tool for studies of the local structure, Proceedings, XVth General Assembly of the European Seismological Commission, Krakow, September 1976, in press.

Berteussen, K.-A.: Moho depth determinations based on spectral ratio analysis of NORSAR long period P-waves, Phys. Earth Planet. Inter., in press.

Berteussen, K.-A., and H. Bungum: Surface wave investigations at NORSAR, Norges Geologiske Undersøkelse series, Geotraverse project, in press.

Berteussen, K.-A., E.S. Husebye, R.F. Mereu and A. Ram: Quantitative assessment of the crust-upper mantle heterogeneities beneath the Gauribidanur Seismic Array in southern India, submitted for publication.

Bungum, H.: Two focal mechanism solutions for earthquakes from Iceland and Svalbard, Tectonophysics, in press.

Bungum, H., T. Risbo and E. Hjortenberg: Precise continuous monitoring of seismic velocity variations and their possible connection to solid earth tides, submitted for publication.

Bungum, H., and E.S. Husebye: The seismicity of Fennoscandia, the Norwegian Sea and adjacent area, Norges Geologiske Undersøkelse series, Geotraverse Project, in press.

Fyen, J., and A. Christoffersson: Weighted array beamforming using non-negative weights, submitted for publication.

Husebye, E.S., R.A.W. Haddon and D.W. King: Precursors to P'P' and upper mantle discontinuities, J. Geophys., in press.

Ringdal, F., and E.S. Husebye: Seismic mapping of heterogeneities in the Fennoscandian lithosphere and asthenosphere using primarily NORSAR array data, Norges Geologiske Undersøkelse series, in press.

Ringdal, F.: P-wave amplitudes and sources of scattering in m_b observations, J. Geophys., in press.

Sandvin, O.A., and D. Tjøstheim: Autoregressive modelling of seismic storms, Proceedings, XVth General Assembly, European Seismological Commission, Krakow, September 1976, in press.

Tjøstheim, D.: Improved seismic discrimination using pattern recognition, submitted for publication.

L.B. Tronrud

VI.2 Program Documentation

No program documentation has been written during this period.

D. Rieber-Mohn

VII SUMMARY OF SPECIAL TECHNICAL REPORTS/PAPERS PREPARED

VII.1 NORSAR Moho Depths from Spectral Ratio Analysis of Long Period P-waves

Using the spectral ratio method discussed by Berteussen (1976), we have tried to estimate Moho depths under NORSAR. In the processing of the data there were several problems which we had to consider. From the simulation done (Berteussen, 1976) we expected that a shortening of the window length used in the calculation of the spectra should imply a sort of smoothing of the spectral ratios. For the real data we did, however, observe that in a number of cases such a shortening implied an unsystematic movement or change in the peaks that can bias the results seriously if care is not taken in the interpretation. Avoiding all cases where such problems occurred, we ended up with 112 spectral ratio estimates. Using the size of the main spectral peak, we estimated the average crustal P-velocity for a one-layer model to be 6.6 km/s. From the shape of the spectral ratios we calculated depth to Moho only, as the variation in the ratio across the array made it obvious that it would be impossible to find a more detailed model. The Moho depths found were then plotted on a diagram of the array at the point where the respective signals were expected to cross Moho. The data showed up to be consistent in that we could not find drastically different depth values plotted close to each other. Thus a signal coming from a certain direction recorded at one instrument gave approximately the same Moho depth as a signal from another direction crossing Moho at the same location and being recorded at another instrument. Smoothing the data and making depth contours we then get the Moho interface displayed on Fig. VII.1.1. For more details see Berteussen (1977). This interface agrees well with the interface calculated by Berteussen (1975) which minimized the short period teleseismic P-wave travel time residuals measured at NORSAR, in that it tends to be deep on the western part of the array (down to 38 km) and shallower (32 km) on the eastern and especially southeastern part of it. It also agrees principally with the structures found by Aki et al (1977) for the area under NORSAR using their block model.

K.-A. Berteussen

REFERENCES

Aki, K., A. Christoffersson and E.S. Husebye (1977): Determination of the three-dimensional seismic structure of the lithosphere, J. Geophys. Res., 82, 277-296.

Berteussen, K.-A. (1975): Crustal structure and P-wave travel time anomalies at NORSAR, J. Geophys. 41, 71-84.

Berteussen, K.-A. (1976): Long period P-wave spectra as a tool for studies of local structures, NORSAR Scientific Report No. 1-76/77.

Berteussen, K.-A. (1977): Moho depth determinations based on spectral ratio analysis of NORSAR long period P-waves, Phys. Earth Planet. Inter., in press.

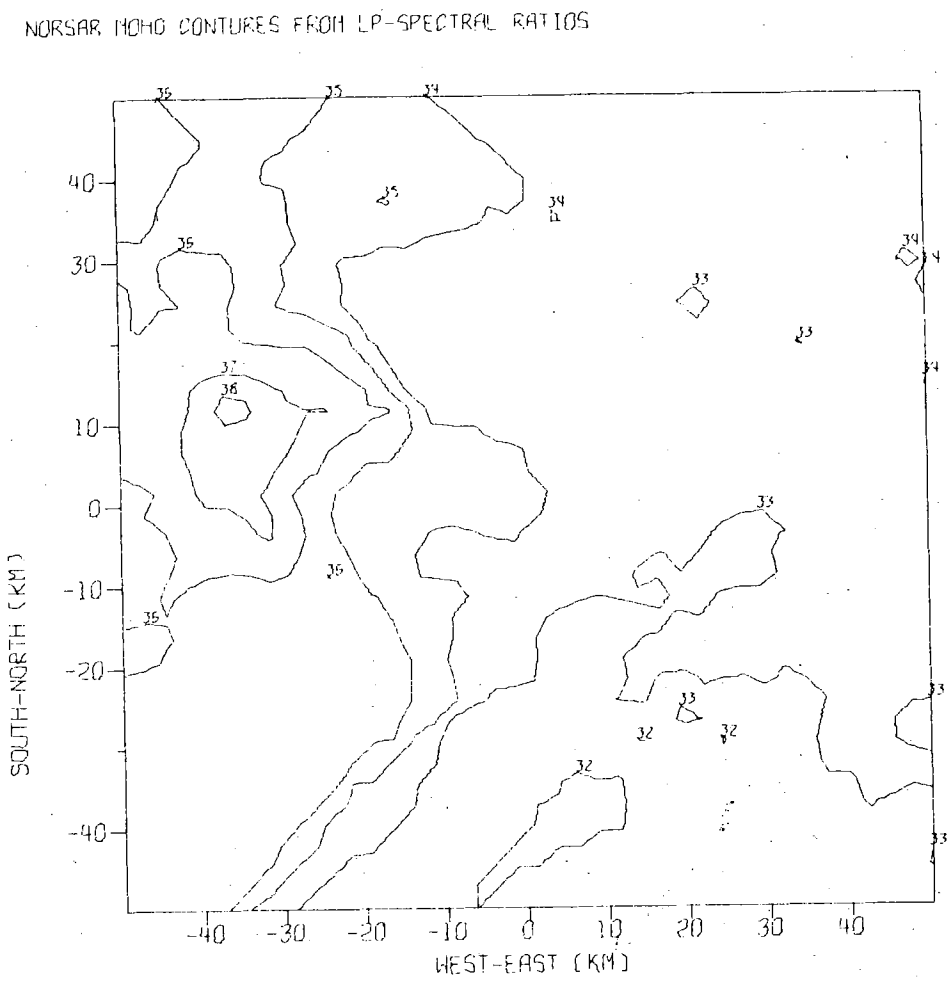

Fig. VII.1.1 NORSAR Moho depth contours estimated from spectral ratio analysis of long period P-waves.

VII.2 Modelling of P-wave Amplitude Anomalies in Terms of Heterogeneities in the Lithosphere

The novel block-inversion scheme of Aki, Christoffersson and Husebye (1977) has proved very successful in analysis of relative travel time observations across an array or network of seismic stations. On the other hand, most efforts aimed at explaining P-wave amplitude anomalies have only been moderately successful. At NORSAR due consideration has been given to this kind of problem in view of their importance for seismic discrimination and at the same time reflecting the need for a better understanding of wave propagation effects of lithospheric heterogeneities. The first step in this direction was a comprehensive mapping of all subarray amplitude anomalies for all beam locations (Berteussen and Husebye, 1974; Berteussen, 1975). The next step was aimed at computing theoretical amplitude distributions across the NORSAR array, and then comparing them with the observational data. In this respect we have used a simplified model for the 3-dimensional structure beneath NORSAR the construction of which was based on the following assumptions: (1) The essential 3-D structures responsible for the observed large-scale amplitude and time anomalies are located in a single layer at a mean depth D below the surface; (2) That P-waves entering this layer from below may be treated as plane waves with uniform amplitude in the plane of the wave; (3) The scales of the inhomogeneities are such that ray theory may be applied; (4) P to S conversions and anelastic effects may be ignored. We further assume that so far as the travel time and amplitude anomalies are concerned the postulated inhomogeneous layer may be treated as an equivalent thin lens located at the mean depth D of the inhomogeneities. This thin lens model was subsequently constructed by projecting travel time residuals for all subarrays for about 200 earthquakes at various depths ranging from 50 to 250 km and then averaging. This time residual model was then converted to the equivalent velocity anomaly model and

then Claerbout's (1976) approach was used for numerical calculation of the wave field on the free surface.

The results obtained so far are very encouraging, i.e., the differences between observed and calculated P-wave amplitudes are generally very small. Even more startling results have been obtained when reversing the above procedure, that is, we have been able to reproduce in great detail the observed travel time residual field from the amplitude anomaly observations via a modified version of Poisson's differential equation.

A comprehensive documentation of this work will be completed in the near future.

R.A.W. Haddon, Sydney University
E.S. Husebye

REFERENCES

Aki, K., A. Christoffersson and E.S. Husebye (1977): Determination of the three-dimensional seismic structure of the lithosphere, J. Geophys. Res., 82, 277-296.

Berteussen, K.-A. (1975): Crustal structure and P-wave travel time anomalies at NORSAR, J. Geophys., 41, 71-84.

Berteussen, K.-A., and E.S. Husebye (1974): Amplitude pattern effects on NORSAR P-wave detectability, NORSAR Scientific Report No. 1-74/75, NTNF/NORSAR, Kjeller, Norway.

Claerbout, J. (1976): Fundamentals of Geophysical Data Processing, McGraw-Hill, New York.

VII.3 The Use of Converted Phases to Infer the Depth of the Lithosphere-Asthenosphere Boundary beneath the Baltic Shield

Long period (2-20 s), longitudinally polarized precursors to direct S have been observed at the NORSAR array from large earthquakes at epicentral distances of 70^{o}-82^{o}. Normal phases, including multiple surface reflections, can be excluded on the basis of slowness and travel time. The slowness of these precursors differs enough from that of the background that the arrival time can be determined to within a second from the resulting discontinuity in the particle motion. The determined slowness (approximately that of direct S) and differential travel time (~28 s relative to S) suggest the interpretation of these arrivals as Sp; the S-to-P refraction is at an approximately horizontal interface about 235 km below the Baltic Shield 2^{o}-3^{o} from NORSAR. The relative polarity of Sp and S (in pahse on the horizontal, out of phase on the vertical) indicates a velocity decrease with increasing depth across the interface. We therefore suggest that the discontinuity is the lithosphere-asthenosphere boundary.

J.A. Snoke, Carnegie Institute, Washington
I.S. Sacks, -"-
E.S. Husebye

VII.4 Two New Earthquake Focal Mechanism Solutions

As a part of our investigations of the seismicity of the North Atlantic Ocean and of the Greenland and Norwegian Seas, focal mechanism solutions have been obtained for two recent earthquakes, one from Iceland and one from Svalbard. A complete report will be published elsewhere (Bungum, 1977).

Iceland Earthquake of 13 January 1976

The PDE solution for this earthquake is based on 160 observations and given as 66.2°N, 16.6°W, with origin time 13.29.19.5 and magnitude 6.0. The focal mechanism solution presented in Fig. VII.4.1 is based on 81 first motion readings from predominantly long period and broad band seismograms. The present focal mechanism solution is in general agreement with those published for an earthquake from 28 March 1963 (Sykes, 1967) and one from 5 May 1969 (Conant, 1972), all situated at or close to the Tjørnes Fracture Zone. We suggest that the actual plane of faulting for the present earthquake is the one striking at 131°, the movement is thereby right-lateral, which is in accordance with the concept of transform faulting. In comparing the strike angles for these three earthquakes, we find a systematic increase as we move from west to east along the fracture zone. Such deviations, which also have been observed along the Jan Mayen Fracture Zone (Bungum and Husebye, 1977), would be consistent with the interpretation of the Tjørnes Fracture zone as an én-echelon system of north-south trending troughs and volcanic chains, developed successively as spreading axes across the fracture zone (Sæmundsson, 1974).

Svalbard Earthquake of 18 January 1976

The PDE solution for this earthquake is based on 128 observations given as 77.9°N, 18.6°E, with origin time 04.46.24.4 and magnitude 5.6. The focal mechanism solution presented in Fig. VII.4.2 is based on 61 first motion readings from

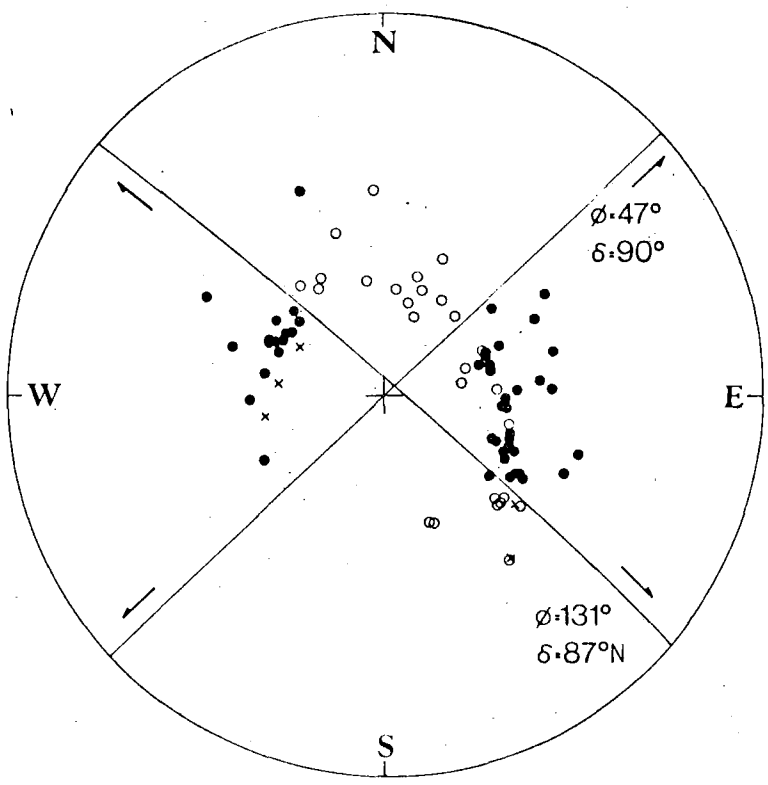

Fig. VII.4.1 Focal mechanism solution for the Iceland earthquake of 13 January 1976. Solid circles are compressions, open circles dilatations, and crosses indicate stations with questionable first motion.

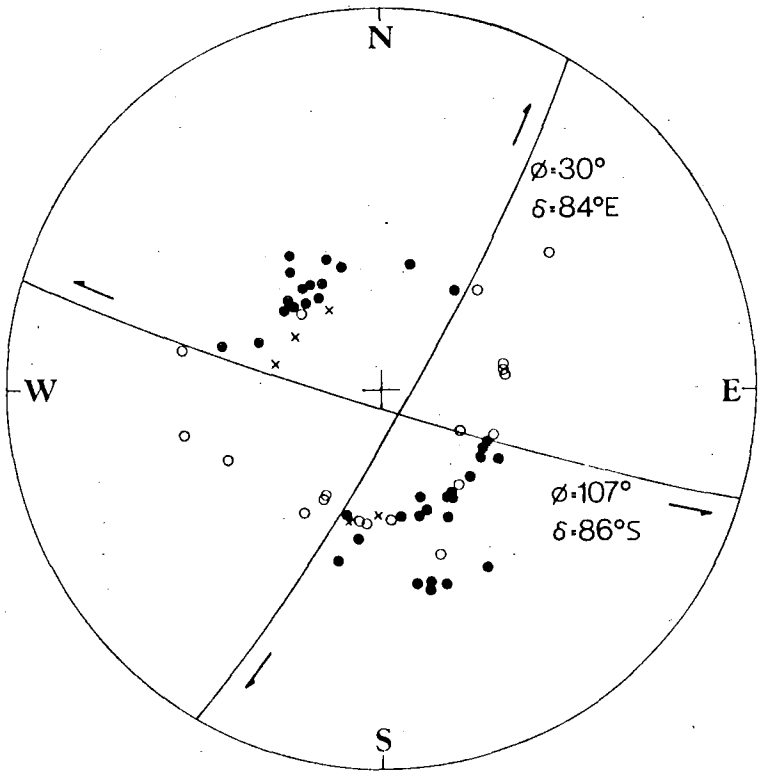

Fig. VII.4.2 Focal mechanism solution for the Svalbard earthquake of 18 January 1976. Solid circles are compressions, open circles dilatations, and crosses indicate stations with questionable first motion.

predominantly long period or broad band seismograms. This is the first focal mechanism solution published for the Svalbard area, and it is noteworthy that a clear strike-slip solution has been obtained for this intra-plate earthquake. Little information is available bearing on the stress pattern in this area, most likely it is the accumulated contribution from several sources and orogenic cycles. The geologic trend in the area (notably late Caledonian and Devonian faulting) is NNW-SSE, and this is just between the directions of the two nodal planes in Fig. VII.4.2. We return briefly to this event in Section VII.5.

H. Bungum

REFERENCES

Bungum, H. (1977): Two focal-mechanism solutions for earthquakes from Iceland and Svalbard. Tectonophysics, in press.

Bungum, H., and E.S. Husebye (1977): Seismicity of the Norwegian Sea: The Jan Mayen Fracture Zone. Tectonophysics, in press.

Conant, D.A. (1972): Six new focal mechanism solutions for the Arctic and a center of rotation for plate movements. M.A. Thesis, Columbia Univ., New York, 18 pp.

Sæmundsson, K. (1974): Evolution of the axial rifting zone in northern Iceland and the Tjørnes Fracture Zone. Geol. Soc. Am. Bull., 85, 495-504.

Sykes, L.R. (1967): Mechanism of earthquakes and nature of faulting on the mid-oceanic ridge. J. Geophys. Res., 72(8), 2131-2151.

VII.5 Seismicity and Crustal Structure in the Svalbard Area

The seismicity of the Svalbard area, characterized by a definite continental structure, is interesting on account of its proximity to the active Knipovich spreading ridge and also in view of the complicated tectonic history of the area in question. We have re-examined the seismic activity here, resulting in the seismicity map presented in Fig. VII.5.1. The map covers the time period 1957-1975, the epicenters are from ISC, PDE and Sykes (1965) (and in that order of priority if more than one of these have reported the event), and only events with at least 6 reporting stations are accepted. The map also contains seven fault plane solutions from the area. The area covered in Fig. VII.5.1 includes the northern part of Mohns Ridge (MR), Knipovich Ridge (KR), Spitsbergen Fracture Zone (SFZ) and the southern part of Nansen Ridge. The seismic activity along Mohns Ridge east of the Greenwich meridian follows the ridge fairly closely, and the normal faulting of Event 5 also confirms this typical behavior for an active spreading axis (Sykes, 1967). The well-organized earthquake pattern extends through the area where the axis 'bends' into the Knipovich Ridge, which is in accordance with the observed continuity between the two ridges (Talwani and Eldholm, in press). The seismicity along Knipovich Ridge is more uneven and dispersed, and the strike-slip solution of Event 1 may suggest movements along a very local fracture zone. The earthquake activity around the Spitsbergen Fracture Zone is also quite dispersed, which has been used as indication for an én-echelon structure of this transform fault (Husebye et al, 1975). It is noticeable that the 3 events for which focal mechanism solutions are available (Events 2-4 in Fig. VII.5.1), have strike directions coincident with those of the fracture zone.

The intraplate seismicity in Fig. VII.5.1 is confined to two areas, the north-east coast of Greenland (with the normal faulting of Event 6) and the Svalbard region. It is seen from

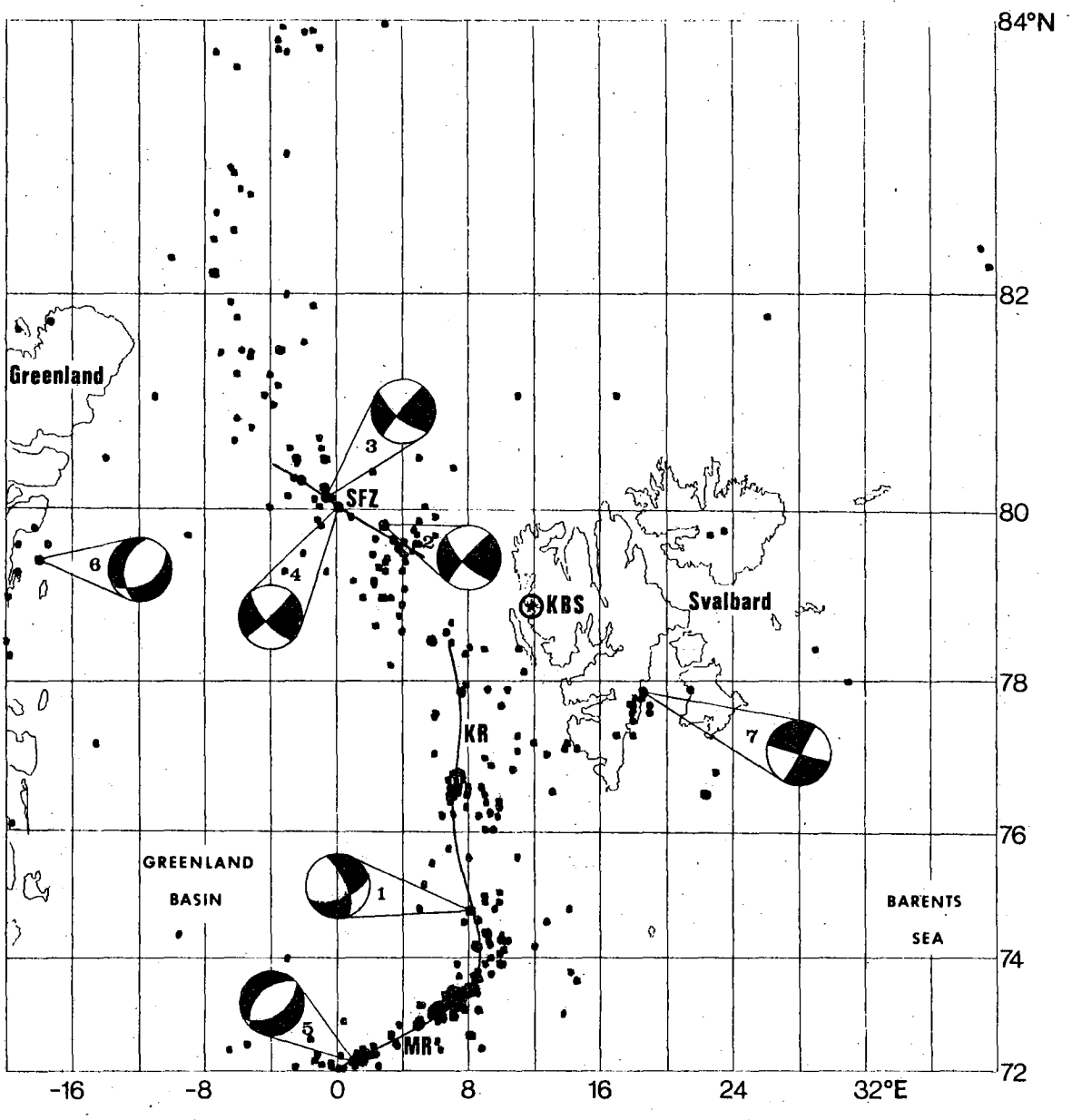

Fig. VII.5.1 Earthquake occurrence in the Greenland/Svalbard region. Only epicentral solutions based on at least 6 stations are used, and the larger symbols indicate a magnitude of at least 5.0. Black and white areas for the seven focal mechanism solutions indicate areas of compression and dilatation, respectively. The structural information on Mohns Ridge (MR), Knipovich Ridge (KR), and the Spitsbergen Fracture Zone (SFZ) is taken from Talwani and Eldholm (in press).

Fig. VII.5.1 that the earthquake activity in the latter area is weak, with the exception of a cluster of events along the southeastern coast of the Spitsbergen island, where a NE-SW trend is observed. A puzzling feature of the seismic activity here is the focal mechanism solution for Event 7, presented in Section VII.4. The available tectonic information cannot resolve the ambiguity of the solution, as the main trend of the Spitsbergen geology is NNW-SSE and thus just between the directions of the two nodal planes. However, the seismicity information give some support for suggesting that the focal plane is the one trending NE-SW, since that direction coincides with the lineation of the earthquake epicenters in the area.

In the second part of this study we have used data from the WWSSN station KBS (see Fig. VII.5.1) in an investigation of the lithospheric structure in the Svalbard area. To this end the spectral ratio method has been employed for estimating local crustal thickness (Phinney, 1964; Berteussen, in press). We scanned all the KBS data for the years 1972-73 and found 8 events suitable for analysis. The observed spectral ratios for these events (calculated for frequencies up to 0.2 Hz) were found to fit the theoretically expected values best for Moho depths around 27 km. In fact, there were two events with 26, one with 27 and five with 28 km. However, since the spectral ratio is also dependent on factors which are kept constant in our calculations (in particular the signal window length and the velocity-depth function), we cannot claim a precision any better than ± 2 km in our determination of the depth to Moho under the station KBS at Svalbard.

H. Bungum
E.S. Husebye
K.-A. Berteussen

REFERENCES

Berteussen, K.-A. (in press): Moho depth determinations based on spectral ratio analysis of NORSAR long period P-waves.

Husebye, E.S., H. Gjøystdal, H. Bungum and O. Eldholm (1975): The seismicity of the Norwegian and Greenland Seas and adjacent continental shelf area. Tectonophysics, 26, 55-70.

Phinney, R.A. (1964): Structure of the earth's crust from spectral behavior of long-period body waves, J. Geophys. Res., 62, 301-324.

Sykes, L.R. (1965): The seismicity of the Arctic. Bull. Seism. Soc. Am., 55, 501-518.

Sykes, L.R. (1967): Mechanism of earthquakes and nature of faulting on the mid-oceanic ridges. J. Geophys. Res., 72, 2131-2153.

Talwani, M., and O. Eldholm (in press): Evolution of the Norwegian-Greenland Sea. Geol. Soc. Am. Bull.

VII.6 A Case Study of Plates in Collision, the Lithosphere in the Hindu-Kush and Pamir Region

It has been recognized for several years that the Hindu Kush region contains a zone of anomalous seismicity which is not readily explained by any simple geometry of plate convergence. The shallow seismicity is most probably associated with the large-scale thrusting exhibited in the Himalayan orogeny, but beneath this lies an intermediate zone of very localized seismicity, perhaps 25 km wide and 300 km long, trending 45° from the shallow zone. We present a delineation of this zone by seismicity data, examine the regional P-wave velocity structure using 2 separate methods. The first of these uses the now familiar 3-dimensional velocity modelling procedure of Aki, Christoffersson and Husebye on arrival time data from a network of stations in the Pamir to produce a localized picture of the velocity structure in the anomalous seismic zone. The change in direction of the seismicity at around 150 km depth is echoed by an abrupt change in the velocity anomaly lineations in the same depth range. The projections to depths of 100 to 200 km of arrival time residuals at a group of more widely spaced WWSSN stations are used to augment the small-scale 3-D structure obtained by the first method with a less detailed, but large scale, 2-D model.

E.S. Husebye
P.C. England, Cambridge University
A.A. Lukk, Institute of Physics of the Earth, Moscow
L.P. Vinnik, -"-

REFERENCES

Aki, K., A. Christoffersson and E.S. Husebye (1977): Determination of the three-dimensional seismic structure of the lithosphere, J. Geophy. Res., 82, 277-296.

VII.7 P-wave Detectability Study of Existing World-Wide Seismograph Stations

A detailed knowledge of the event detection capabilities of existing seismograph stations is a prerequisite in order to accurately assess the existing capabilities for monitoring underground nuclear explosions. Such information can most reliably be obtained by actually measuring the performance of each station over an extended period of time, in terms of the number of reported teleseismic events. The method of Ringdal (1975) is well suited to this kind of analysis, provided an adequate 'reference system' (i.e., an organization reporting a comprehensive event catalogue and associated magnitudes) is available. In this respect, an analysis of the event detection capabilities of seismograph stations in Fennoscandia was undertaken by Pirhonen et al (1976), based upon ISC reported events during the years 1964-69. Fig. VII.7.1 shows the type of results obtained by this study, and the excellent fit of the detection curves shows that the resulting detectability estimates must be considered very reliable.

The objective of the present study, which is as yet in its initial stage, is to perform a comprehensive evaluation of world-wide P-wave detectability of existing seismograph stations in terms of ISC magnitude. The incremental probability G of detection, given event magnitude m, is assumed to be of the form (Ringdal, 1975)

$$G(m;\mu,\sigma) = \int_{-\infty}^{m} \frac{1}{\sqrt{2\pi}\cdot\sigma} \cdot \exp(-(x-\mu)^2/(2\sigma^2))\ dx \qquad (1)$$

where the two parameters μ and σ characterize the detection capability. Assuming, for a given station, that the probability of 'false alarm' is equal to V_F, and the probability of the

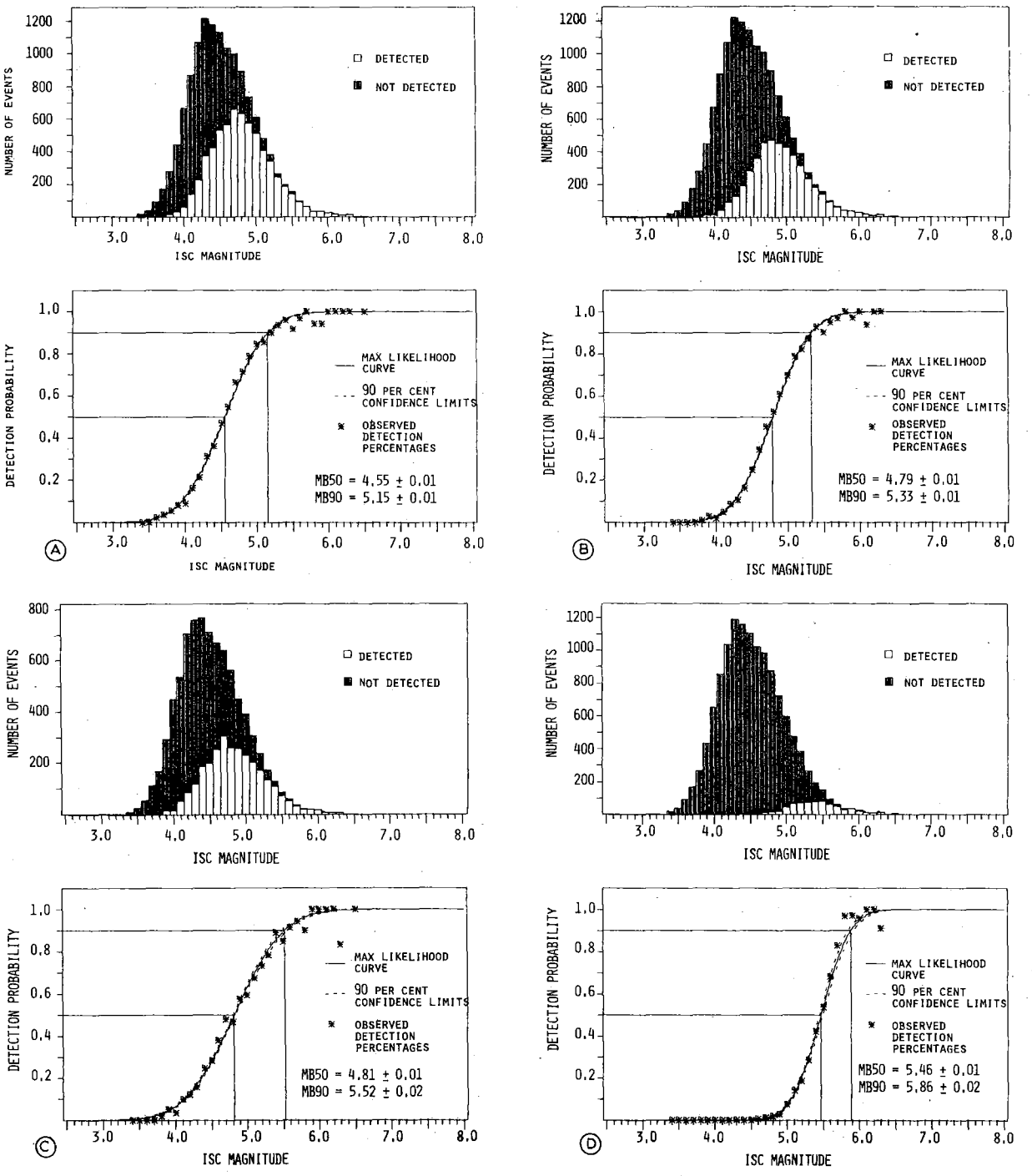

Fig. VII.7.1 Teleseismic (30^{o}-90^{o}) P-wave detection statistics for selected stations based on the years 1964-69. The upper half is a histogram showing the reference event set and the number of events actually detected for each magnitude. the lower half shows the maximum likelihood detectability curve and its confidence limits. The actual percentage of detected events at each magnitude is also shown.

A. For station NUR (Nurmijarvi, Finland
B. For station UPP (Uppsala, Sweden)
C. For LHN (Lillehammer, Norway)
D. For COP (Copenhagen, Denmark)

station being out of operation is equal to V_D, it follows that the probability of finding a station detection that can be associated to a given event of ISC magnitude m is:

$$P(m)=P(m;\mu,\sigma,V_F,V_D)=(1-V_D)\cdot[V_F+(1-V_F)\cdot G(m;\mu,\sigma)] \quad (2)$$

For a given set S of reference events, denote by D the set of indices for which the station actually has a detection. The logarithm of the associated likelihood function then becomes (Ringdal, 1975)

$$\log L(\mu,\sigma,V_F,V_D) = \sum_{i\in D} P(m_i) + \sum_{i\notin D} (1-P(m_i)) \quad (3)$$

This function may subsequently be maximized to obtain maximum likelihood estimates of the parameters μ,σ,V_F,V_D. In practice, V_F may reasonably be set to 0, since the chance of a 'random association' in the ISC bulletin can be considered very small. However, the 'downtime' parameter V_D cannot in general be ignored, and must be estimated on the basis of available data. We note in passing that Pirhonen et al (1976) estimated V_D directly from operational statistics obtained from the Fenno-scandian stations; however, this procedure cannot be used in the present case as no reliable operational reports are generally available.

Our initial detectability results, as presented here, have been obtained by, for each station reporting to the ISC, extracting those ISC reported events that have been located within 30-90 degrees epicentral distance of the station. Only events with an associated ISC computed m_b value have been used in this reference set. Table 1 summarizes the observed detection percentages and the estimated 50 and 90 per cent incremental teleseismic detection thresholds for a subset of 96 stations. This subset consists of those stations with an estimated 50 per cent threshold of m_b=5.0 and better.

STATION NAME AND LOCATION		LAT LON	DETECTION PERCENTAGE AT ISC MB 3.5	4.0	4.5	5.0	5.5	6.0	6.5	*****OBSERVED***** DET	TOT	PC	MAVG	***ESTIMATED*** M50	M90	UPTM
AAB -TALGAR	KAZAKHSTAN	43.16N, 77.23E	0	4	22	56	80	89	79	2312	6069	38	5.07	4.80	5.41	85
ALE -ALERT	NORTHWEST TERRITORY	82.29N, 62.24W	2	8	29	68	94	94	89	1786	4310	41	4.95	4.73	5.36	95
ALQ -ALBUQUERQUE	NEW MEXICO	34.56N,106.27W	0	4	22	56	78	75	90	1282	3878	33	4.98	4.76	5.34	80
ARE -AREQUIPA	PERU	16.27S, 71.29W	0	1	13	47	85	85	100	307	1036	30	5.07	4.95	5.49	90
ASP -ALICE SPRINGS	NORTHERN TERRITORY	23.41S,133.53E	24	23	49	81	95	96	82	2377	3832	62	4.92	4.44	5.16	95
BDF -BRASILIA ARRAY (W)	BRAZIL	15.39S, 47.54W	11	14	28	51	59	68	100	520	1485	35	4.84	4.63	5.56	70
BKR -BAKURIANI	GEORGIA,USSR	41.44N, 43.31E	4	3	20	53	81	84	78	1181	3411	35	5.06	4.89	5.53	90
BLC -BAKER LAKE	NORTHWEST TERRITORY	64.19N, 96. 1W	0	5	19	52	80	90	80	1302	4275	30	4.99	4.90	5.58	90
BMO -BLUE MOUNTAINS	OREGON	44.50N,117.18W	71	77	87	91	98	90	92	3939	4527	87	4.67	0.0	0.0	90
BNG -BANGUI	CENTRAL AFRICA REP.	4.22N, 18.34E	6	31	55	68	71	71	50	1083	1883	58	4.79	4.08	4.72	70
BOD -BODAYBO	CENTRAL SIBERIA	57.51N,114.11E	0	4	19	45	73	73	73	1181	3310	36	5.10	4.89	5.60	80
BRG -BERGGIESSHUBEL	GERMANY	50.52N, 13.56E	0	1	13	34	42	49	50	685	3582	19	5.00	4.66	5.09	40
BRS -BRISBANE	QUEENSLAND	27.23S,152.46E	0	3	15	47	80	96	88	1057	3184	33	5.12	5.00	5.66	95
BUL -BULAWAYO	RHODESIA	20. 8S, 28.36E	0	7	36	76	96	98	100	1035	1943	53	4.96	4.67	5.28	100
CIR -CHIREDZI	RHODESIA	21. 0S, 31.34E	0	1	25	58	83	95	50	717	1757	41	5.02	4.81	5.42	90
CLL -COLLM BERG	GERMANY	51.18N, 13. 0E	0	12	39	78	97	96	88	1785	3607	49	4.91	4.58	5.17	95
COL -COLLEGE OUTPOST	ALASKA	64.54N,147.47W	16	29	56	84	93	91	94	3265	4994	65	4.88	4.29	4.97	90
CPO -CUMBERLAND PLATEAU	TENNESSEE	35.35N, 85.34W	4	19	37	71	92	94	88	1483	3122	48	4.87	4.62	5.41	95
CTA -CHARTERS TOWERS	QUEENSLAND	20. 5S,146.15E	0	8	28	61	92	95	88	1584	3596	44	5.02	4.78	5.45	95
DUG -DUGWAY	UTAH	40.11N,112.48W	0	9	27	59	77	76	90	1600	4323	37	4.92	4.69	5.37	80
EDM -EDMONTON	ALBERTA	53.13N,113.21W	4	14	44	77	90	89	90	2189	4368	50	4.86	4.51	5.13	90
EIL -EILAT	ISRAEL	29.33N, 34.57E	0	0	8	33	54	52	43	559	2918	19	5.11	4.90	5.38	55
EKA -ESKDALEMUIR ARRAY	SCOTLAND	55.19N, 3. 9W	3	2	11	43	77	81	78	909	3732	24	5.10	4.99	5.57	85
ELT -YELTSOVKA	WESTERN SIBERIA	53.15N, 86.16E	0	6	27	58	79	79	77	1704	4188	41	5.03	4.70	5.31	80
EUR -EUREKA	NEVADA	39.29N,115.58W	9	28	54	80	89	90	85	2691	4510	60	4.81	4.32	5.08	90
FAY -FAYETTEVILLE	ARKANSAS	36. 7N, 94.11W	0	1	7	48	85	86	78	781	3272	24	5.14	4.98	5.44	90
FCC -FORT CHURCHILL	MANITOBA	58.45N, 94. 5W	4	5	16	46	77	83	90	1173	4349	27	5.00	4.99	5.73	90
FFC -FLIN FLON	MANITOBA	54.43N,101.58W	8	15	37	70	88	90	80	1898	4240	45	4.85	4.60	5.34	90
GBA -GAURIBIDANUR ARRAY	INDIA	13.36N, 77.26E	0	4	17	48	75	86	93	1269	3780	34	5.11	4.97	5.67	90
GIL -GILMORE CREEK	ALASKA	64.58N,147.29W	4	12	39	71	87	95	100	2569	4985	52	4.96	4.58	5.25	90
GMA -GRANITE MOUNTAIN	ALASKA	65.25N,161.13W	2	6	24	57	82	90	88	1986	4973	40	5.04	4.82	5.50	90
GOL -GOLDEN	COLORADO	39.42N,105.22W	0	3	11	38	61	67	60	824	3918	21	5.03	4.98	5.65	70
GRF -GRAFENBERG ARRAY	GERMANY	49.41N, 11.12E	0	8	29	64	82	85	89	1399	3569	39	4.94	4.69	5.32	85
HFS -HAGFORS	SWEDEN	60. 8N, 13.41E	37	46	60	82	96	94	88	2506	3762	67	4.76	4.16	5.41	100
IFR -IFRANE	MOROCCO	33.31N, 5. 7W	0	3	11	42	73	72	75	592	2377	25	5.04	4.97	5.58	80
ILT -IULTIN	NORTH-WEST SIBERIA	67.54N,178.42W	0	5	20	45	76	83	82	1614	4716	34	5.08	4.97	5.73	90
IMA -INDIAN MOUNTAIN	ALASKA	66. 4N,153.40W	0	8	16	34	42	51	47	1202	4929	24	4.98	4.74	5.59	50
INK -INUVIK	NORTHWEST TERRITORY	68.17N,133.30W	0	12	29	58	83	84	70	1786	4452	40	4.94	4.77	5.58	90
JAS -JAMESTOWN	CALIFORNIA	37.56N,120.26W	0	3	19	63	96	97	92	1805	4770	38	5.05	4.82	5.34	95
JCT -JUNCTION CITY	TEXAS	30.28N, 99.48W	6	3	13	41	65	68	56	812	3374	24	5.03	4.91	5.54	70
KBL -KABUL	AFGHANISTAN	34.32N, 69. 2E	16	23	44	68	74	78	64	2061	3973	52	4.90	4.39	5.27	80
KEV -KEVO	FINLAND	69.45N, 27. 0E	0	4	15	50	87	98	88	1302	4273	30	5.07	4.99	5.65	100
KHC -KASPERSKE HORY	CZECHOSLOVAKIA	49. 7N, 13.34E	0	10	38	77	97	95	89	1731	3548	49	4.93	4.60	5.18	95
KHO -KHOROG	TADZHIKISTAN	37.29N, 71.32E	0	3	15	42	68	75	57	1171	3995	29	5.10	4.91	5.54	75
KIC -KOSAN BOKA	IVORY COAST	6.21N, 4.44W	4	28	50	79	86	84	80	1438	2490	58	4.80	4.38	5.15	90
KIR -KIRUNA	SWEDEN	67.50N, 20.25E	5	10	31	68	92	95	88	1786	4129	43	4.94	4.70	5.37	95
KJF -KAJAANI	FINLAND	64.11N, 27.42E	11	20	50	83	96	96	88	2280	3888	59	4.87	4.44	5.10	95
KRA -CRACOW	POLAND	50. 3N, 19.56E	0	1	10	53	89	96	86	949	3307	29	5.14	4.92	5.36	90
KRR -KAROI	RHODESIA	16.51S, 29.37E	0	2	26	61	84	95	100	690	1660	42	5.01	4.78	5.37	90
KRV -KIROVABAD	AZERBAYDZHAN	40.39N, 46.20E	0	3	14	41	66	84	70	939	3415	27	5.09	4.99	5.69	80

Table VII. 7.1

Teleseismic (30°-90°) P-wave detection capability of selected stations reporting to the ISC during 1971-73. The following items are listed: (i) station code, (ii) geographical coordinates, (iii) percentage of detected reference events in magnitude bins of 0.5 m_b units centered at 3.5, 4.0, etc., (iv) total number of detected events, reference events and corresponding percentage detected, (v) average ISC reported m_b of the detected events, (vi) estimated 50 and 90 per cent incremental detection threshold, (vii) estimated percentage of total time when the station was actually reporting.

ISC STATIONS DETECTABILITY STUDY 1971-1973 NTNF/NORSAR

STATION NAME AND LOCATION		LAT LON	DETECTION PERCENTAGE AT ISC MB 3.5	4.0	4.5	5.0	5.5	6.0	6.5	*****OBSERVED***** DET	TOT	PC	MAVG	***ESTIMATED*** M50	M90	UPTM
LAO -LASA CENTRE	MONTANA	46.41N,106.13W	91	90	83	77	81	74	80	3514	4247	83	4.50	0.0	0.0	80
LBF -LES BUTEAUX	FRANCE	46.59N, 3.58E	0	2	12	50	85	82	70	959	3485	28	5.10	4.94	5.47	90
LOR -LORMES	FRANCE	47.16N, 3.51E	0	2	13	54	91	89	80	1040	3503	30	5.10	4.90	5.39	90
LPB -LA PAZ	BOLIVIA	16.31S, 68. 5W	11	17	50	77	93	89	100	611	1050	58	4.87	4.44	5.11	90
MAT -MATSUSHIRO	HONSHU	36.32N,138.12E	0	4	20	59	93	97	92	1579	3412	46	5.13	4.85	5.40	95
MBC -MOULD BAY	NORTHWEST TERRITORY	76.14N,119.21W	15	30	50	69	83	82	80	2287	4235	54	4.79	4.38	5.49	90
MOX -MOXA	GERMANY	50.38N, 11.36E	3	7	31	75	97	96	88	1601	3595	45	4.96	4.67	5.22	95
MTD -MOUNT DARWIN	RHODESIA	16.46S, 31.35E	0	1	18	37	56	62	0	425	1555	27	5.00	4.82	5.48	60
NAO -NORSAR A	NORWAY	60.49N, 10.49E	45	59	50	45	47	55	63	1886	3756	50	4.60	0.0	0.0	50
NDI -NEW DELHI	INDIA	28.41N, 77.13E	0	2	13	45	82	90	93	1241	3981	31	5.16	4.98	5.56	90
NEW -NEWPORT	WASHINGTON	48.15N,117. 7W	0	6	24	65	95	96	91	1729	4546	38	4.98	4.78	5.36	95
NIE -NIEDZICA	POLAND	49.25N, 20.19E	0	2	17	51	75	69	71	969	3301	29	5.04	4.80	5.30	75
NIL -NILORE	PAKISTAN	33.39N, 73.15E	0	4	20	44	62	61	64	1206	3957	30	5.04	4.77	5.43	65
NTI -NORDMAN	IDAHO	48.37N,116.57W	0	3	17	54	85	90	80	1402	4541	31	5.03	4.88	5.46	90
NUR -NURMIJARVI	FINLAND	60.30N, 24.39E	9	24	51	83	98	99	88	2145	3601	60	4.86	4.46	5.22	100
OBN -OBNINSK	CENTRAL RUSSIA	55.10N, 36.36E	0	2	20	63	92	93	88	1374	3547	39	5.07	4.79	5.28	90
PMR -PALMER	ALASKA	61.35N,149. 7W	2	5	28	65	89	95	100	2309	5156	45	5.04	4.76	5.37	95
PNS -PENAS	BOLIVIA	16.16S, 68.28W	11	24	54	81	92	89	100	646	1047	62	4.84	4.36	5.04	90
PNT -PENTICTON	BRITISH COLUMBIA	49.19N,119.37W	2	3	16	53	89	92	91	1417	4620	31	5.05	4.89	5.46	90
PRE -PRETORIA	SOUTH AFRICA	25.45S, 28.11E	0	1	14	46	78	80	100	613	1968	31	5.07	4.90	5.44	80
PRU -PRUHONICE	CZECHOSLOVAKIA	49.59N, 14.32E	0	4	22	68	92	97	88	1344	3542	38	5.03	4.75	5.24	90
QUE -QUETTA	PAKISTAN	30.11N, 66.57E	0	5	25	61	82	82	79	1592	3914	41	5.04	4.74	5.32	85
ROL -ROLLA	MISSOURI	37.55N, 91.52W	0	2	9	24	34	38	33	457	3343	14	4.98	4.89	5.57	40
SES -SUFFIELD	ALBERTA	50.23N,111. 2W	4	8	33	71	92	90	91	1873	4395	43	4.91	4.65	5.24	90
SHI -SHIRAZ	PERSIA	29.38N, 52.31E	0	3	15	53	86	93	91	1182	3391	35	5.12	4.89	5.44	90
SHL -SHILLONG	INDIA	25.34N, 91.53E	0	1	10	38	63	73	82	1075	4183	26	5.16	4.95	5.50	70
SOD -SODANKYLA	FINLAND	67.22N, 26.37E	5	20	46	80	97	99	88	2293	4098	56	4.88	4.53	5.28	100
SOP -SOPRON	HUNGARY	47.41N, 16.33E	0	1	7	25	42	46	50	488	3353	15	5.08	4.93	5.48	45
SPA -SOUTH POLE	ANTARCTICA	90. 0S, 0. 0E	0	36	55	68	75	70	92	1752	2762	63	4.96	4.04	4.97	75
SSF -SAINT-SAULGE	FRANCE	47. 3N, 3.30E	0	2	12	51	86	82	80	981	3475	28	5.09	4.93	5.46	90
SVE -SVERDLOVSK	WESTERN SIBERIA	56.48N, 60.38E	0	1	14	45	71	81	90	1053	3640	29	5.13	4.93	5.51	80
TAM -TAMANRASSETT	ALGERIA	22.47N, 5.31E	0	10	24	42	49	61	67	645	2093	31	4.88	4.68	5.58	60
TCF -TOULX-STE-CROIX	FRANCE	46.17N, 2.12E	0	2	10	48	76	69	60	863	3418	25	5.09	4.92	5.44	80
TIK -TIKSI	EASTERN SIBERIA	71.38N,128.52E	0	4	21	49	73	80	82	1438	4000	36	5.08	4.83	5.49	80
TTA -TATALINA	ALASKA	62.55N,156. 1W	0	1	7	21	34	44	41	737	5056	15	5.12	4.97	5.61	40
TUC -TUCSON	ARIZONA	32.18N,110.46W	0	5	22	62	93	89	90	1491	4055	37	5.01	4.78	5.33	90
TUL -TULSA	OKLAHOMA	35.54N, 95.47W	0	13	35	70	88	92	89	1469	3274	45	4.89	4.62	5.29	90
UBO -UINTA BASIN ARRAY	UTAH	40.19N,109.34W	45	47	55	60	58	51	60	2309	4216	55	4.66	0.0	0.0	60
UME -UMEA	SWEDEN	63.48N, 20.14E	13	16	37	69	93	96	88	1843	3868	48	4.90	4.68	5.52	100
UPP -UPPSALA	SWEDEN	59.51N, 17.37E	8	10	30	68	95	99	88	1617	3768	43	4.96	4.75	5.46	100
UZH -UZHGOROD	UKRAINE	48.38N, 22.18E	0	0	7	41	79	80	86	756	3311	23	5.18	4.98	5.44	80
VAN -VANNOVSKAYA	TURKMENIYA	37.57N, 58. 6E	0	0	3	18	33	34	18	390	3464	11	5.20	4.98	5.44	35
WRA -WARRAMUNGA ARRAY	NORTHERN TERRITORY	19.56S,134.20E	20	27	51	76	92	92	82	2337	3828	61	4.90	4.36	5.17	90
YAK -YAKUTSK	EASTERN SIBERIA	62. 1N,129.43E	0	1	13	34	55	72	40	941	3460	27	5.14	4.96	5.63	65
YKC -YELLOW KNIFE	NORTHWEST TERRITORY	62.28N,114.28W	2	8	20	52	81	80	80	1321	4228	31	4.96	4.90	5.66	90
ZAK -ZAKAMENSK	CENTRAL SIBERIA	50.23N,103.17E	0	4	19	52	76	81	79	1443	3911	37	5.09	4.82	5.43	80

Table VII.7.1 (cont.)

For four stations (NORSAR, LASA, UBO, BMO) no estimates have been given due to the fact that these stations detect essentially all ISC events in the appropriate distance range, hence ISC is not suitable as a reference network in these cases. Otherwise we note that stations of high detectability are found worldwide; e.g., Africa (BNG; m_{50}=4.1, KIC -4.4), South America (PNS - 4.4; BDF - 4.6), Antarctica (SPA - 4.0), Asia (KBL - 4.4; ELT - 4.7), Australia (ASP - 4.4; WRA - 4.4), besides several sensitive stations in North America and Europe.

Future work on the detectability study will concentrate on evaluating the potential bias in ISC m_b estimates and its effects on our detectability computations. Also, a possible regionalization of detection thresholds will be studied. Moreover, an analysis will be undertaken in order to determine to what extent the detection of a given event by stations within a close distance of one another are correlated. This is important since global detectability studies (e.g., Snell, 1976) generally assume statistical independence in this context.

F. Ringdal
E.S. Husebye
J. Fyen

REFERENCES

Pirhonen, S.E., F. Ringdal and K.-A. Berteussen (1976): Event detectability of seismograph stations in Fennoscandia. Phys. Earth Planet. Int., 12, 329-342.

Ringdal, F. (1975): On the estimation of seismic detection thresholds. Bull. Seism. Soc. Am., 65, 1631-1642.

Snell, N.S. (1976): Network capability estimation, Texas Instruments Report No. ALEX(01)-TR-76-04, Dallas, Texas.

VII.8 Autoregressive Modelling of Seismic Storms

A nonstationary autoregressive (AR) time series model given by

$$X(t) - a_1(t)\, X(t-1) - \ldots - a_{p(t)}\, X(t-p) = Z(t) \qquad (1)$$

has been fitted to the long period (LP) noise registered at NORSAR. Here $X(t)$ is the observed LP-noise while $Z(t)$ is a white noise residual process satisfying $E\{Z(t)\ \overline{Z(s)}\}=\sigma_z^2(t)\delta_{ts}$. The LP-noise is assumed to be approximately stationary within time intervals of duration 5 min. (300 samples), and time variation of the coefficients is introduced by fitting stationary models to a sequence of such intervals. The corresponding spectra are completely described by the AR coefficients and the variance σ_z^2, and are given by

$$P(f) = \frac{2\sigma_z^2}{\left|1-\sum_{k=1}^{p} a_k \exp(-2\pi i f k)\right|^2} \qquad 0 \leq f \leq \tfrac{1}{2} \qquad (2)$$

The order $p=p(t)$ of the model has been estimated using the Final Prediction Error criterion and is a function of time. The time variation of the spectrum is now determined by the behavior in time of $a_1(t),\ldots,a_{p(t)}(t)$ and $\sigma_z^2(t)$. Usually the time variation is described in terms of selected spectral peaks, but this leads to loss of information.

The autoregressive modelling was used to examine the changes in the LP-spectrum during two microseismic storms described by Korhonen and Pirhonen (1976). The first example is a cyclone center over the North Sea in the time period March 20-25 1972. An AR-model of order 7 produced a satisfactory approximation to the spectrum. However, most of the spectral information is contained in the first two coefficients. The white noise variance σ_z^2 acts as a scaling factor. The time development

of the coefficient $\hat{a}_1$ and the variance $\hat{\sigma}_z^2$ for the vertical component of the LP-noise is shown in Fig. VII.8.1 a) and b) respectively. The parameter $\hat{\sigma}_z^2$ has a sharp peak on March 23 at about 18h00 for all three components. This corresponds to the maximum power of the first and second peak (Korhonen and Pirhonen, 1976) of the vertical component spectrum. It is also interesting to note that the wind velocity has a maximum between March 22 and March 23, which corresponds to the time interval of greatest change for the coefficient $\hat{a}_1$. For more details and for a discussion of the second example (a cyclone center approaching the North Atlantic in the time interval May 24-27 1972) we refer to Sandvin and Tjøstheim (1977).

O.A. Sandvin
D. Tjøstheim

REFERENCES

Korhonen, H., and S.E. Pirhonen (1976): Spectral properties and source areas of storm microseisms at NORSAR. Scientific Report No. 2-75/76, NTNF/NORSAR, Kjeller, Norway.

Sandvin, O.A., and D. Tjøstheim (1977): Autoregressive modelling of seismic storms. Proceedings, 15th General Assembly of European Seismological Commission, Krakow, 22-28 September 1976, to appear.

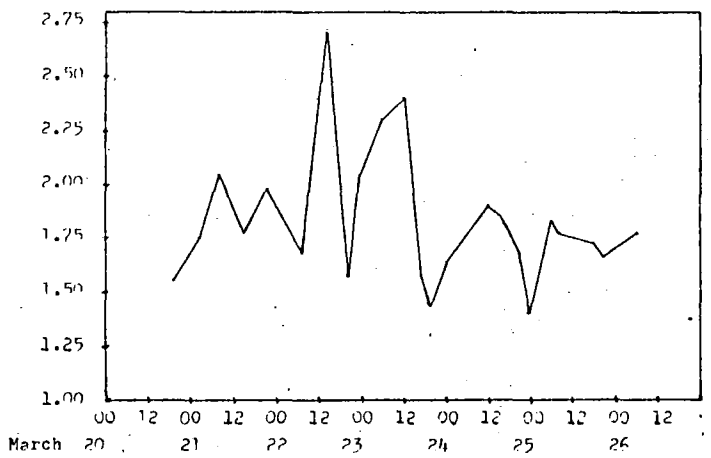

a)

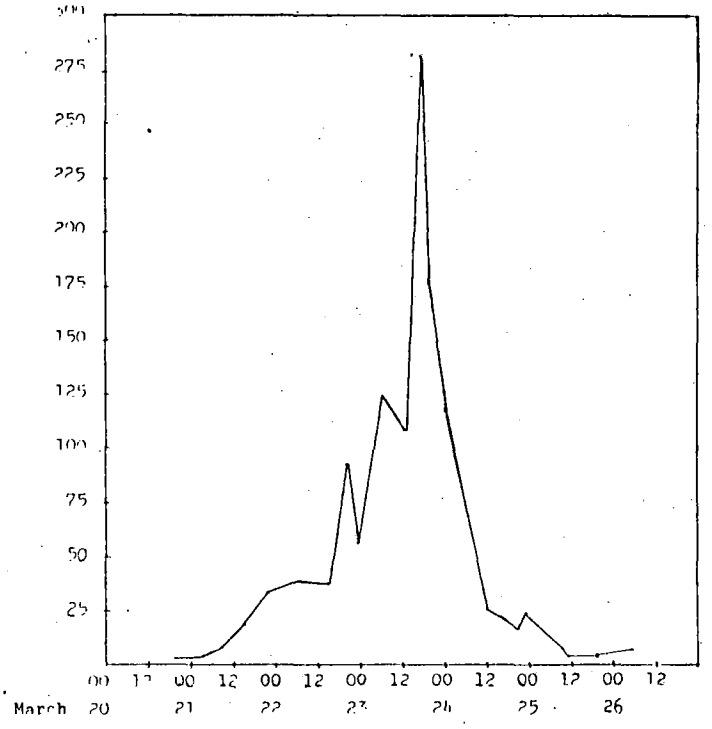

b)

Fig. VII.8.1 a) Variation of coefficient $\hat{a}_1$ for vertical LP-noise from subarray 01A.

b) Variation of variance parameter $\hat{\sigma}_z^2$ for vertical LP-noise from subarray 01A.

VII.9 A Pattern Recognition Approach to Seismic Discrimination. Part II: Classification

As explained in Part I (Tjøstheim, 1976) the seismic discrimination problem, when identified as a pattern recognition problem, can be separated into two stages: feature extraction and classification. The construction of a primary feature vector $\underline{Y}$ containing short and long period features was described in Tjøstheim (1976). Using principal component analysis the vector $\underline{Y}$ has been further reduced to an 8-dimensional feature vector $\underline{Z}$ where

$$\underline{Z} = [Z_{EX}(1), \ldots, Z_{EX}(4); Z_{EQ}(1), \ldots, Z_{EQ}(4)] \qquad (1)$$

with

$$Z_{EX}(i) = \underline{Y} \cdot \hat{\underline{h}}^{T}_{i,EX} \qquad (2)$$

where $\hat{\underline{h}}_{i,EX}$, i=1,...,4 are the four major estimated principal component vectors of the explosion data set. The quantities $Z_{EQ}(i)$, i=1,...,4 are defined similarly.

It is assumed that the $\underline{Z}$ vector is governed by a multivariate Gaussian probability density function $P_1(z)$ or $P_2(z)$ corresponding to the explosion (1) population or earthquake (2) population. The density function estimation problem then reduces to estimating the respective mean vectors and covariance matrices. The following decision rule was applied: For a given observed event with a corresponding feature vector $\underline{Z}$, the quantities $P_1(\underline{Z})$ and $P_2(\underline{Z})$ were computed, and $\underline{Z}$ was assigned to the population i having the largest probability $P_i(\underline{Z})$ of having $\underline{Z}$ occurring.

In practice this means that the decision rule is to declare an explosion if $\hat{S}_1(\underline{Z}) - \hat{S}_2(\underline{Z})$ is positive and an earthquake if this difference is negative. Here

$$S_i(\underline{Z}) = -\tfrac{1}{2} \log|\hat{R}_i| - \tfrac{1}{2}(\underline{Z}-\hat{\underline{\mu}}_i)\ \hat{R}_i^{-1}(\underline{Z}-\hat{\underline{\mu}}_i)^T \qquad (3)$$

where $\hat{R}_i$ and $\hat{\underline{\mu}}_i$, i=1,2 are the explosion and earthquake $\underline{Z}$-vector covariance matrices and mean vectors respectively. This classification rule was applied on the data set of 52 explosions and 73 earthquakes described in Tjøstheim (1976). The results are displayed in the bottom part of Fig. VII.9.1 where the events have been plotted according to their value of $\hat{S}_1(\cdot)-\hat{S}_2(\cdot)$. It is seen that all events are correctly classified.

For matters of comparison we treated the m_b:M_s data and the X1:X2 discriminant data of Tjøstheim and Husebye (1976) in a similar way. That is, we used the discriminant (3) but with $\underline{Z}$ replaced by $\underline{U} = (m_b, M_s)$ or $\underline{V} = (X1, X2)$. (The notation L1:L2 is used on the figure.) From Fig. VII.9.1 it is seen that the m_b:M_s data produces serious overlap and that the performance is clearly inferior to the discriminant based on $\hat{S}_1(\underline{Z})-\hat{S}_2(\underline{Z})$. The X1:X2 data produces complete separation, but with one explosion very close to the explosion-earthquake decision line.

D. Tjøstheim

REFERENCES

Tjøstheim, D. (1976): A pattern recognition approach to seismic discrimination Semiannual Technical Summary, NORSAR Sci. Report No. 4-75/76, pp. 36-41.

Tjøstheim, D., and E.S. Husebye (1976): An improved discriminant for test ban verification using short and long period spectral parameters, Geophys. Res. Lett., 3, pp. 499-502.

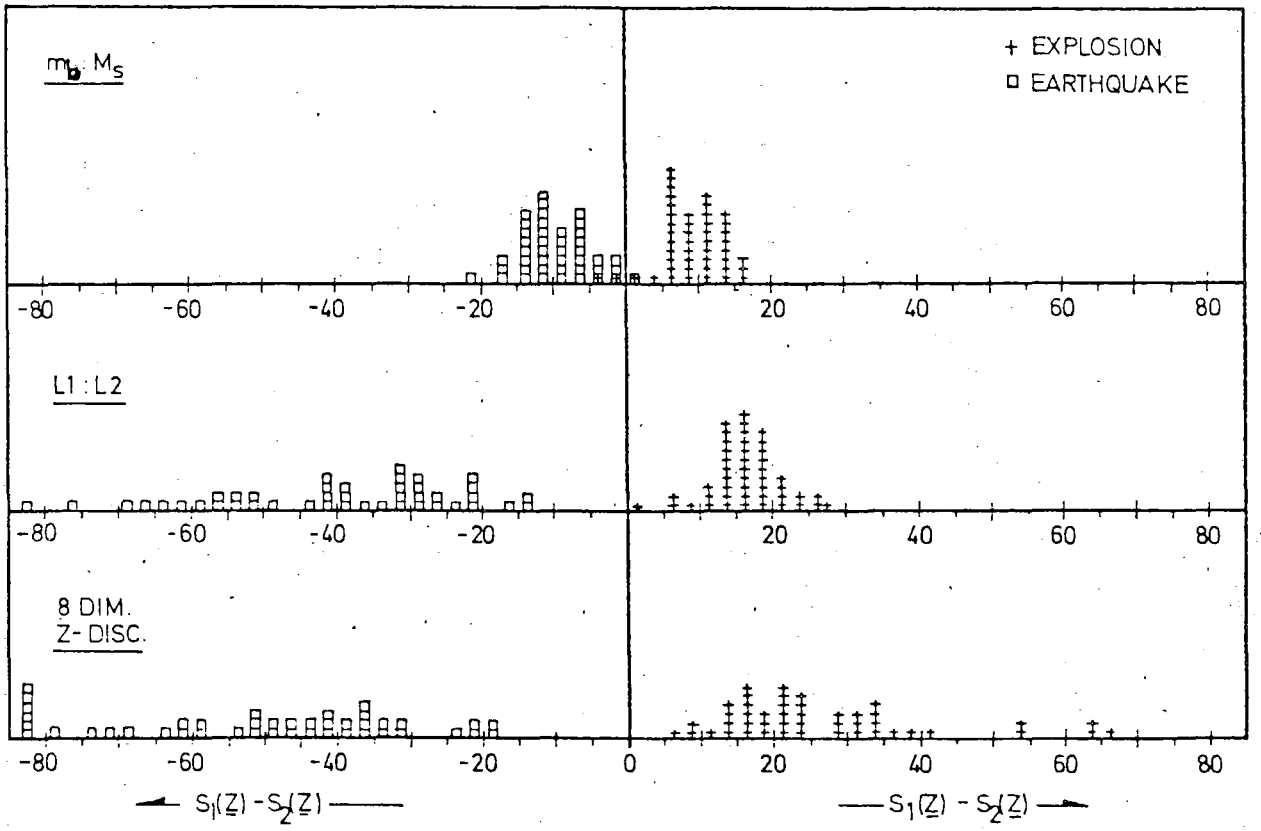

Fig. VII.9.1 Histogram of discrimination scores $S_1(\cdot)-S_2(\cdot)$ as determined by Eq. (3).

VII.10 A New Method of Spectral Estimation for Spatial Data

Geophysical data in general and seismological data in particular are often recorded both in space and in time. While a number of efficient statistical techniques exist for analysis of data observed in time, this is not so for spatial data. We propose here a new type of analysis for spatial variables observed on a grid. The proposed technique might be viewed as a generalization of the time-series autoregressive analysis, but there is also some justification for considering it a spatial extension of Burg's (1975) maximum entropy analysis.

For simplicity consider the case where we have a geophysical quantity $F(x_1,x_2)$ observed on a regular grid in the X_1-X_2 plane. We use the notation $S<x,y]$ for the vectors of integers $u=(u_1,u_2)$ which are such that $x_k \leq u_k \leq y_k$ for $k=1,2$ but $u \neq x$, and seek to model $F(x) = F(x_1,x_2)$ by a one-sided autoregressive model in the plane

$$F(x) - \sum_{y \in S<0,p]} a(y)\, F(x-y) = Z(x) \qquad (1)$$

where $Z(x) = Z(x_1,x_2)$ is a spatial white noise series. Corresponding to the time series case we obtain an estimate $\hat{f}(\lambda) = \hat{f}(\lambda_1,\lambda_2)$ of the two-dimensional power spectral density of $F(x)$ as

$$\hat{f}(\lambda) = \frac{\hat{\sigma}_z^2}{\left|1 - \sum_{y \in S<0,p]} \hat{a}(y)\, \exp\{-i[y,x]\}\right|^2} \qquad (2)$$

We have done some preliminary simulation experiments, using artificially generated data $F(x)$. In each case we computed $\hat{f}(\lambda)$ as well as an FFT power spectral estimate. Fig. VII.10.1 shows the results for a model of the form

$$F(x_1,x_2)=Z(x_1,x_2)+0.85\sigma_z \cos(1.5x_1+1.5x_2)+0.85\sigma_z \cos 1.5x_2 \qquad (3)$$

where we have two cosines embedded in two-dimensional spatial white noise. It is seen that the two spectral peaks are much sharper in the autoregressive case. This suggests that as in the time series case there may be cases where spatial autoregressive procedures are superior to FFT estimates. More tests are required to put this conclusion on a firmer basis.

D. Tjøstheim

REFERENCES

Tjøstheim, D. (1977): Autoregressive modelling and spectral estimation for spatial data. Some simulation experiments. Stanford Exploration Project, Department of Geophysics, Stanford University, Progress Report Vol. 11, to appear.

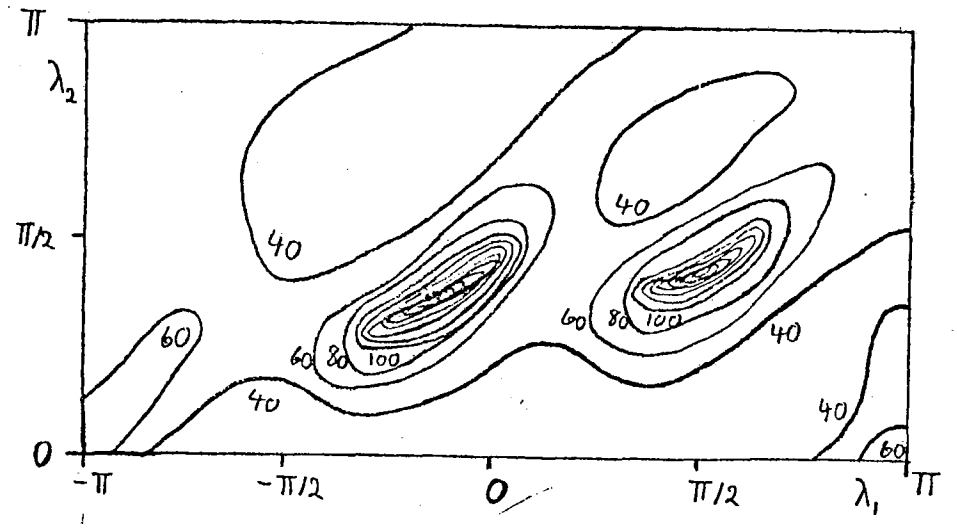

(a)

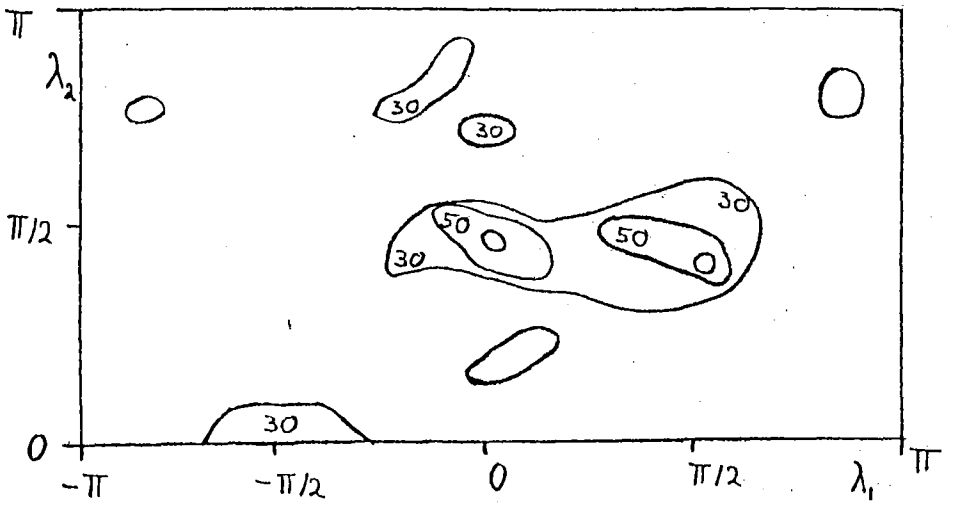

(b)

Fig. VII.10.1 Autoregressive AR(3,3) spectral approximation (a) and FFT approximation (b) of cosines embedded in spatial white noise.

VII.11 Estimating the Autocorrelation Function of Spatio-Temporal Variables

In geological exploration as well as in air pollution studies it is often necessary to interpolate from a sparse and irregularly positioned set of measurement points. The principal practical difficulty (Delfiner, 1976) in studies of this sort consists in obtaining good estimates for the spatial autocorrelation function. Motivated by these problems we suggest (Tjøstheim, 1977) an estimate for the autocorrelation function for spatio-temporal variables. The estimate is meaningful for non-integer lags and for irregularly positioned data points. It is constructed using a double Fourier transform technique. The statistical properties of the estimate are studied in a special case. For more details and for a brief summary of applications to air pollution modelling, we refer to Tjøstheim (1977).

D. Tjøstheim

REFERENCES

Delfiner, P. (1976): Linear estimation of nonstationary spatial phenomena, Proceedings of NATO A.S.I. "Geostatistics 75", Rome, Italy. Reidel Publ. Corp., Dordrecht, The Netherlands.

Tjøstheim, D. (1977): On the problem of estimating the autocorrelation function of spatio-temporal variables, Dept. of Statistics, Stanford University, SIMS Tech. Report, to appear.